Predator-prey interactions under thermal pressure

A thesis presented to

The Faculty of Graduate Studies

of

Lakehead University

by

Ryley Marchant

In partial fulfillment of requirements

for the degree of

Master of Science in Biology

September 5, 2025

© Ryley Marchant, 2025

Abstract

Ectotherms' ecological performance is directly linked to their thermal environment, many of which are warming due to climate change. If predator and prey thermal niches differ, warming may impact the intensity of predator-prey interactions, with subsequent effects on their populations. To determine how warming may impact predator-prey interactions, I fit and compared maximum swim speed thermal performance curves (TPCs) of Dytiscidae predaceous diving beetles (Tribe Agabini) and their prey, Wood Frog (*Lithobates sylvaticus*) and Eastern Gray Treefrog (*Dryophytes versicolor*) tadpoles. I then used climate change projections and measures of pond water temperature to determine how relative swim speeds of predators and prey may change in the future. Due to a lack of predicted future water temperature data, I established an air-water temperature relationship by fitting a generalized linear model (GLM) to 2024 air and water temperatures from 5 sites north of Thunder Bay, Ontario. I then used predicted air temperature data for 2025-2100 and my GLMs to get predicted water temperatures for the next 75 years. TPC comparisons between Agabini predators and tadpole prey revealed that predators have a performance advantage over *D. versicolor* tadpoles at warmer temperatures, but not *L. sylvaticus* tadpoles. Agabini beetle thermal optimum (T_{opt}) (28.6 ± 1.6 ºC) was also significantly greater than *D. versicolor* (24.2 ± 0.9 ºC, $p = 0.025$), but not significantly different from *L. sylvaticus* (25.7 ± 3.2 ºC, $p = 0.163$). Agabini beetle 80% thermal tolerance breadth ($T_{br(80\%)}$) (13.5 ± 0.9) was significantly narrower than *D. versicolor* (18.1 ± 0.9, $p = 0.040$) but not significantly different from *L. sylvaticus* (19.1 ± 2.7, $p = 0.162$). Predictions showed that pond temperatures will increase through time, giving Agabini beetle predators an increasing performance advantage over *D. versicolor*

over the next 75 years. However, due to similar performance measures between *L. sylvaticus* and the predators, their interaction will not be impacted by temperature changes over the next 75 years. These results show variability between predator-prey pairs in the same environment. When the predator's performance advantage over their prey increases, it may result in increased predation pressure and reduced prey populations, while other predator-prey interactions will be unaffected. Thus, as climate change alters thermal regimes, predator-prey interactions will be altered, but not between all predator-prey pairs.

Acknowledgements

Over the course of this project, many people have played a role in enabling its success and completion. I am very grateful for you all.

I would like to start by thanking my supervisor, Dr. Adam Algar. I consider myself incredibly lucky to have had such a supportive and thoughtful supervisor. Your guidance, encouragement, and understanding were invaluable throughout this process, and I can say without a doubt that I would not have completed this degree without you. You challenged me to tackle unfamiliar territory (R), persevere through hours of video and photo analysis, and take initiative in areas I knew well, such as field and lab work. I am also very thankful for the opportunity to be part of the Lakehead University Ectotherm Ecology and Evolution Lab.

I would also like to extend my sincere thanks to my committee members, Dr. Steve Hecnar and Dr. Lesley Lancaster, for their advice and insightful feedback throughout the project. A special thank you goes to my field assistant, Scarlett Hanley. Your willingness to spend long days in the field and at the Biology Aquatics Facility, along with your great ideas, laughter, and steady companionship, made this experience far more enjoyable and productive.

Thank you to Sarah Leduchowski for the dedicated care you provided to the tadpoles used in this study, and to Dr. Rick Relyea for your methodological guidance. I'd also like to thank Dr. Ladislav Malek, Dr. Azim Mallik, Dr. Kam Leung, and Dr. Susanne Walford for generously lending equipment and space for this project. Thank you to Loch Lomond

Ski Hill, Kamview Nordic Centre, and my Nanny, Lynda Lambert, for allowing me to collect animals on your properties.

To everyone in the Lakehead University Ectotherm Ecology and Evolution Lab — thank you for listening to countless practice presentations, offering constructive feedback, and being a consistent source of support. I am especially grateful to Melissa Henderson for listening to many of my frustrations, helping troubleshoot problems, and encouraging me to keep going during difficult times.

To my friends — thank you for your patience and understanding each time I said, “Sorry, I’m busy,” and for your continued support from afar.

To my best friend and greatest supporter, Tomasz — thank you for being by my side for the past eight years. Your unwavering belief in me has encouraged me to take on challenges, and your constant support has helped me push through them. Your love, encouragement, and on-demand iced coffees have been invaluable throughout this journey, and I truly could not have made it here without you.

To my parents — thank you for always supporting my education and encouraging me to follow my goals. You’ve taught me that I can achieve anything I put my mind to, and you've been there with financial help, emotional support, and endless study snacks. I truly appreciate everything you've done.

Finally, to my beloved animal companions — my horse, Gem, and my dog, Ellie — thank you for your unconditional love, for giving me a reason to leave my desk and get outside, and for all the emotional support I could ever ask for.

Land Acknowledgment

I would like to acknowledge that this research has taken place on the traditional lands of Indigenous peoples. With this acknowledgment I seek to honour Indigenous people and this land.

Field work for my study took place on the traditional lands of the Anishinaabe and Ojibwe peoples and is signatory to Treaty 3 and the Robinson Superior Treaty of 1850. This region includes lands stewarded by the Lac La Croix, Seine River, Nigigoonsiminikaaning, and Fort William First Nations, among others.

I recognize and respect Indigenous Nations and their inherent rights to this land. I express deep gratitude for the opportunity to live and work on this land, and I commit to ongoing learning, listening, and meaningful action that honours Indigenous histories, voices, and futures.

Table of Contents

List of Tables

List of Figures

1 Introduction

1.1 Background

Climate change is among the strongest drivers of physiological and geographical change seen in flora and fauna worldwide (Deutsch *et al.* 2008; Parmesan & Yohe 2003; Poloczanska *et al.* 2013). Species are thermally vulnerable to climate change when they become exposed to thermal regimes outside of their thermal niche, i.e. the range of body temperatures in which population growth is above zero (Gvoždík 2018). Thermal extremes cause stress to organisms and result in a range of consequences, from temporarily decreased performance to death (Buckley & Huey 2016). A substantial body of research has focused on assessing direct impacts of future climate change on species' thermal vulnerability (Buckley *et al.* 2022; Deutsch *et al.* 2008; Huey & Kingsolver 2019; Sunday *et al.* 2014). Such studies can be useful in determining how individual species may respond to abiotic changes. However, less is known about how climate change will impact the complex network of interactions between and within species in a region (Montoya & Raffaelli 2010). It is important to understand how biotic interactions are affected by climate change because of their ecological importance; for example, 'connectance', the proportion of realized trophic interactions among all potential interactions, influences population stability and community dynamics (Petchey *et al.* 2010). Thus, it is vital to deepen our ecological understanding of how climate change will affect biotic interactions, and the consequences of these effects on individuals, populations, species, communities, and ecosystems.

While measuring the direct effect of climate change on organisms is useful, measuring the indirect effects of altered biotic interactions is also key to understanding the full effects of climate change (Gilman *et al.* 2010). Climate change will affect ecological networks, altering the strength of biotic interactions within communities and likely create new interactions as ranges shift (Montoya & Raffaelli 2010). As organisms shift their ranges to track climate change, they may also face increased competition and predation or limited availability of mutualists, making colonization difficult (Eck *et al.* 2014; HilleRisLambers *et al.* 2013; Nagano *et al.* 2023). The strength of biotic interactions may also change due to thermal mismatches between actors. Differences in thermal tolerances of interacting species results in different performance capabilities and behaviours, potentially benefiting or hurting one or both species (Bideault *et al.* 2021; Meehan & Lindo 2023; Pintanel *et al.* 2021). Groups at particular risk to climate change include reptiles, amphibians, and polar invertebrates as they have limited physiological plasticity, restricted latitudinal ranges, and long generation times (Morley *et al.* 2019). These vulnerable species are all ectotherms, which have also been found to have limited ability to acclimate to increased temperatures (Morley *et al.* 2019), further increasing their vulnerability to climate change.

Climate change will alter biotic interactions between organisms with differing thermal tolerances and thermal performance. Ectothermic organisms are exceptionally impacted by climate change because they cannot maintain their body temperatures through metabolic heat production and instead rely on external sources of heat (Angilletta 2009; Guderley 2004). For this reason, ectotherm physiological processes, performance capabilities, and behaviours, are highly dependent on their thermal environment. For

example, tadpole oxygen consumption (Kern *et al.* 2015) and predatory fish swim performance increase with temperature (Öhlund *et al.* 2015), and aphids leave their host plants to avoid heat stress (Ma *et al.* 2018). Because biotic interactions involve two actors, then there is the potential for them to respond differently to changing temperature. For example, if predators have a higher heat tolerance than their prey, or have greater performance at warmer temperatures, climate warming could result in increased predation pressure (Allan *et al.* 2015). Thus, comparing interacting organisms thermal performance or thermal tolerance can give insight into how their interactions may change through time (Pintanel *et al.* 2021; but see Sinclair *et al.* 2016).

1.2 Ectotherm thermal physiology

Internal body temperature is pivotal in an organism's physiological processes, including metabolic reactions, growth, development, and ecological performance (Beachy *et al.* 1999; Cano & Nicieza 2006; Ge *et al.* 2022). For all living organisms, acquired energy is used for biosynthesis (e.g. growth), maintenance (e.g. circulation or respiration), or external work (e.g. locomotion) and then dissipated from their bodies (Careau *et al.* 2014). Ectothermic organisms cannot maintain their body temperatures via metabolic heat production and instead rely on external sources of heat (Angilletta 2009; Guderley 2004). Ectotherms acquire heat through their skin from solar radiation or conduction from warm surfaces, and lose heat through convection with the air or water or latent heat loss (Gates 1980; Tracy 1976). In water, conduction and convection are the main pathways of heat exchange between organisms and their environment, except in the case that they receive direct warming from solar radiation near the water's surface (McDiarmid & Altig 1999). In general, the rate of bodily processes increases with body

temperature, increasing energetic demands and allowing for improved physical performance (Rezende & Bozinovic 2019), until the point of protein denaturation triggering a decline in performance.

Body temperature directly impacts ectotherms' performance (Kern *et al.* 2015). This relationship can be represented using thermal performance curves (TPCs), which quantify how performance (e.g. swim speed, oxygen consumption, digestive rate) varies with body temperature (Sinclair *et al.* 2016). TPCs provide key information on the thermal niche, including thermal optimum (T_{opt}, the temperature of maximum performance), critical thermal limits (CT_{min} and CT_{max}, the minimum and maximum temperatures when organisms lose motor control), and 80% tolerance breadth ($T_{br(80\%)}$, the range of temperatures in which performance is greater than or equal to 80% of the maximal performance); (Figure 1.1). TPCs can be used to predict species vulnerability to climate change (Luhring & DeLong 2016; Payne *et al.* 2016) but should be used with caution as TPCs are often variable throughout ontogeny, acclimation, geographic position, and even between difference performance traits (Sinclair *et al.* 2016).

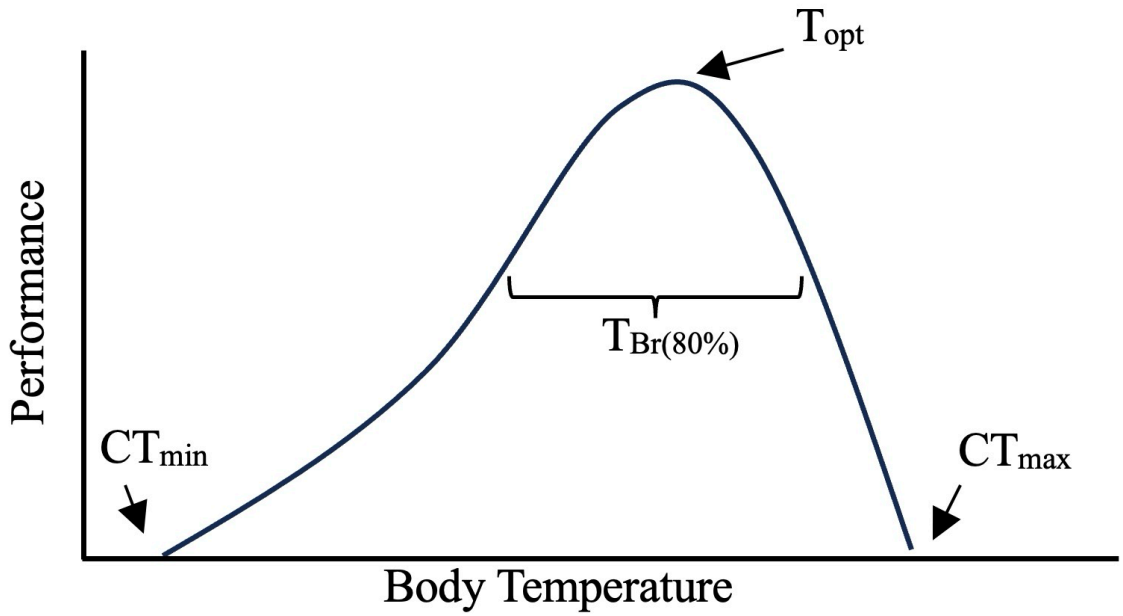

Figure 1.1. Generalized thermal performance curves showing key features. CT_{min} and CT_{max} are the minimum and maximum temperatures that individuals can withstand before they lose bodily control, T_{opt} is the temperature at which the maximum performance occurs, and 80% thermal tolerance breadth ($T_{Br(80\%)}$) is the range of temperatures where performance is greater than or equal to 80% of the maximal performance.

In the face of climate change, aquatic and terrestrial environments are experiencing increasing temperatures, putting thermal stress on the organisms living within them (Häder & Barnes 2019). For example, some organisms in both terrestrial and aquatic environments have limited warming tolerances – a measure of the tolerable temperature increase before reaching their upper thermal limits – that makes them more vulnerable to warming (Morley *et al.* 2019), although definitions and methods between studies are inconsistent (Clusella-Trullas *et al.* 2021). In environments with unfavourable temperatures, organisms can use behavioural thermoregulation, which involves an organism changing its' actions or habitat use to restrict or increase its' exposure to radiation (Ma *et al.* 2018), to help control its body temperature. Thermal heterogeneity in terrestrial and aquatic environments provides a temporary escape from thermal extremes,

however not without consequences. For example, aphids will drop off of their host plant to avoid thermal extremes and take up residency on plants in cooler microhabitats, but this decreases their chances of survival and reproduction (Ma *et al.* 2018). To help reduce the physical harm from exposure to nonoptimal temperatures, individuals can also make physiological adjustments to maximize their performance, for example, acclimatization. Acclimatization is any, usually, reversible physiological adjustment in an organism caused by an altered environment (Lagerspetz 2006). Thermal acclimatization alters the shape and or position of the TPC allowing organisms to achieve higher levels of performance than would be otherwise possible.

1.3 Predator-prey thermal mismatch

Biotic interactions within and across trophic levels affect individual fitness and population dynamics (Bideault *et al.* 2021). Thus, temperature-induced changes in interaction intensity could have broader ecological and biogeographical consequences, though we still have limited understanding of what these may be. Predator-prey interactions have direct impacts on species' population size, distribution, and fitness (Meehan & Lindo 2023), making them an important branch of ecological research. There are different stages of a predator-prey interaction; detection, capture, and handling; and 'body velocity' is a major factor in determining the efficacy and efficiency of each stage (Dell *et al.* 2014). In aquatic systems, swim and burst speeds are often chosen as a measure of thermal performance between predators and prey as they quantify the 'capture' part of their interaction (Allan *et al.* 2015; Grigaltchik *et al.* 2012; Gvoždík & Smolinský 2015). Other methods of measuring predator-prey interaction strength includes direct consumption of prey biomass (Davidson *et al.* 2021), proportion of prey

eaten over a given timeframe (Anderson *et al.* 2001), metabolic rate (Freitas *et al.* 2007), or predator attack rate (Öhlund *et al.* 2015). Some predatory species have been found to benefit from warming, experiencing increased maximum swim speeds, capture success, and predation rates (Allan *et al.* 2015; Grigaltchik *et al.* 2012; Öhlund *et al.* 2015). However, not all predator-prey pairs will be affected in this way. For example, active (Backswimmers) and ambush (damselfly larvae) predators both experienced an increased prey (*Daphnia*) encounter rate as environmental temperatures increase, but, due to faster prey swim speeds, the active predator could not capture the prey but the ambush predator could (Twardochleb *et al.* 2020).

Predator-prey interactions depend on the relative performance of both actors and if their responses to the environmental changes are different, this could lead to altered predation rates and population dynamics. Thermal physiology could differ between predators and prey due to varying methods of energy acquisition, food quality, behaviour, and energy demands (Freitas *et al.* 2007), or varying thermal tolerances (Katzenberger *et al.* 2021; Pintanel *et al.* 2021). Predator energetic efficiency, the ratio between energy inputs (food intake) and energy outputs (metabolism), is temperature dependent and can be visualized using TPCs (Sentis *et al.* 2012). Ectotherms may occupy various trophic levels, and trophic interactions involving only ectothermic organisms will be especially influenced by changes to their thermal environment. Ectotherms, even ones living in the same area, have interspecific variability in thermal tolerances (Savva *et al.* 2018) and may respond differently to the same temperature fluctuations in their environment (Broitman *et al.* 2009). If ectotherms in different trophic levels or niches are responding differently to the same temperature changes, this could impact their biotic interactions

and could have broader impacts on predation rates, prey population density, and species ranges (Pintanel *et al.* 2021).

The relative difference between prey and predator performance at different temperatures can be determined by comparing their TPCs (Figure 1.2). The advantage of the predator at a given temperature (T) can be determined by the difference between prey and predator performance, where predator performance advantage (ΔV_T) is equal to:

$$\Delta V_T = V_{T,\,pred} - V_{T,\,prey}$$

Where $V_{T,\,pred}$ and $V_{T,\,prey}$ are the performance of the predator and prey at temperature T, respectively. Evaluating changes in ΔV_T can provide insight into how potential predation pressure may be affected by temperature changes through time (e.g. due to climate change), or space (e.g. along environmental gradients).

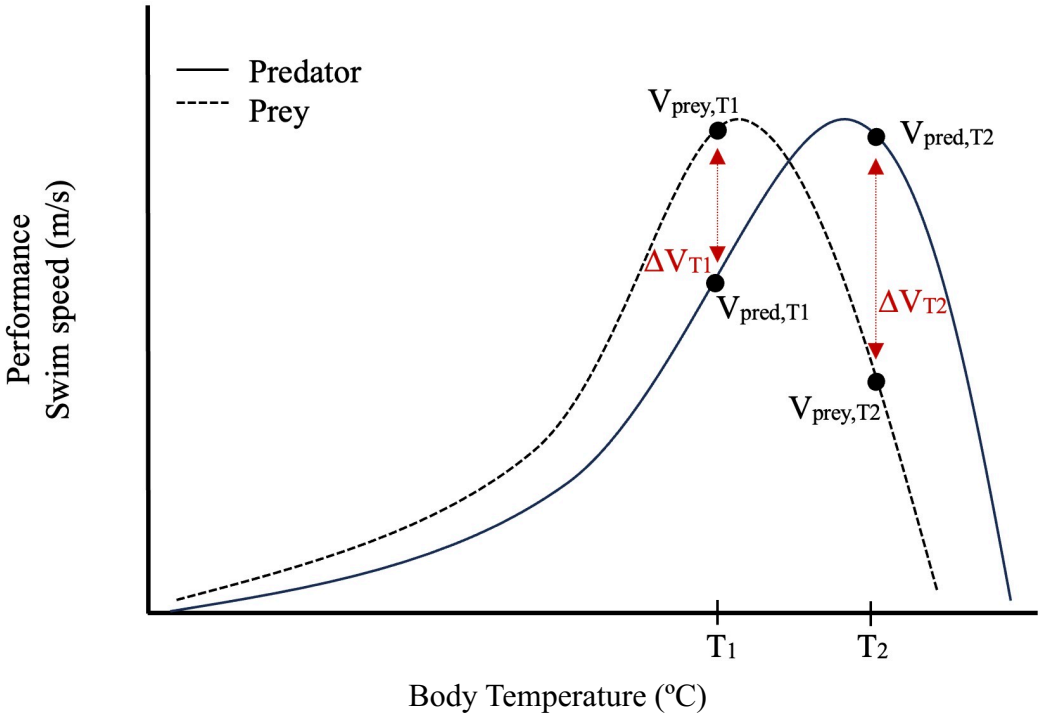

Figure 1.2. Example of how thermal performance curves of organism swim speeds at various temperatures can be used to calculate predator performance advantage (ΔV_T) and infer changes in predator-prey interactions. T_1 represents the current environmental mean temperature and T_2 represents warmer future conditions. $V_{prey,T1}$ and $V_{prey,T2}$ are prey performances at current and future temperatures, respectively. $V_{pred,T1}$ and $V_{pred,T2}$ are predator performances at current and future temperatures, respectively. ΔV_{T1} and ΔV_{T2} are predator advantages at current and future temperatures, respectively.

1.4 Biology of small freshwater ponds

Aquatic environments are vulnerable to climate change because their hydrology depends on precipitation, temperature, ground and surface water resources, evaporation, transpiration, and their physical and biotic features (Leibowitz & Brooks 2007). Climate change will affect almost all those aspects, having a strong influence on aquatic environments and the organisms living in them. A general warming trend has been observed in large water bodies across North America (Schindler 1998), but whether there is a trend for small ephemeral ponds is unknown. However, as climate change is expected to increase summer temperatures, and decrease summer precipitation, ephemeral ponds

are likely to experience shorter hydroperiods, and warmer water temperatures, causing substantial ecological impacts (Brooks 2004, 2005; Brooks & Hayashi 2002; Cartwright *et al.* 2021; Leibowitz & Brooks 2007).

Ectothermic organisms that inhabit small and/or ephemeral ponds, such as tadpoles, larval salamanders, and fully- or semi-aquatic invertebrates are sensitive to changes in their thermal environment (Ohba 2011; Relyea 2001). Tadpoles make an excellent study specimen for thermal physiology studies as they are practically isothermal with their environment, all physiological processes are influenced by temperature, and they are unaffected by confounding processes like dehydration as they are fully aquatic (Lutterschmidt & Hutchison 1997). Tadpole thermal performance has been used to measure developmental rates (Seebacher & Grigalchik 2015), organismal response to climate change (Beltran 2019; Perotti *et al.* 2018), and heritability of traits (Xu *et al.* 2024).

There are a range of aquatic invertebrates that inhabit small ponds and predate tadpoles, such as adult and larval predaceous diving beetles (Dysticidae), larval dragon and damselflies (Odonata), and giant water bugs (Belostomatidae; Dodd 2023; Ohba 2011; Relyea 2001). These predator-prey relationships, involving only ectothermic organisms, have the potential to be heavily influenced by pond water temperatures. Methods of predation in this environment vary; some larval diving beetles are ambush predators, while adult diving beetles are more active and chase their prey (Campbell 1969; Culler *et al.* 2014). As adults chase their prey, their swim performance is directly related to their ability to successfully capture prey. Past work has found that insect predators have higher thermal maximums than anuran prey (Katzenberger *et al.* 2021;

Sunday *et al.* 2014), and that predation rates increase with temperature (De Mira-Mendes *et al.* 2019). Given the dependence of this interaction on swim speed, predators should be able to outperform prey and increase predation rates in warming conditions. Understanding the thermal sensitivity of predator and prey swim speed is a key step to predicting how predation intensity will be impacted by future climate change.

1.5 Hypotheses

In this thesis, I aim to compare swim speed thermal performance curves of two tadpole prey species (Eastern Gray Treefrogs and Wood Frogs) and their Dytiscidae predators (Tribe: Agabini), measure predator performance advantage (ΔV_T), predict future pond water temperatures using predicted climate data and a model of air and water temperatures from 2024, and determine how ΔV_T will change over the next 75 years.

I tested the following hypotheses:

Hypothesis 1: Predators have a performance advantage over their prey at warmer temperatures.

Rationale: Past work has found that insect predators have a higher CT_{max} than amphibian prey, fish predators swim faster than prey at warmer temperatures, and predation rates increase at warmer temperatures (Allan *et al.* 2015; De Mira-Mendes *et al.* 2019).

Prediction: Predator performance, swim speed (m/s), will be greater than prey at warmer temperatures and predators will have a higher T_{opt} and CT_{max} than their prey.

Hypothesis 2: As environmental temperatures increase over the next 75 years, predators will have an increasing performance advantage over their prey.

Rationale: Predators with a performance advantage over prey at warmer temperatures will be benefitted by increasing environmental temperatures over the next 75 years as they will be able to out-perform their prey.

Prediction: Predator performance advantage (ΔV_T) will significantly increase over the next 75 years.

2 Methods

2.1 Study region

Figure 2.1. Locations of study sites. Yellow pins show sites used in final analysis, white pins show sites with insufficient data collected to be used in analysis, purple pin shows a site that was only used in one portion of the analysis. Red circles are the location of cities and townships. and the white circles shows lakes.

Field work was done along a 180 km S–N transect, to the west of Thunder Bay, Ontario, Canada. Pond water temperature (surface and bottom) and air temperature were recorded at 11 sites (Figure 2.1); the transect started just north of the USA border and ran

north to west of Lake Nipigon. In June, average air temperatures of Upsala (just west of this transect) and Thunder Bay (just east) were 21 °C and 19 °C, respectively. The transect ran through the Lake Nipigon (3W) and Pigeon River (4W) ecoregions (Crins *et al.* 2009). These regions have a mean summer rainfall of 231–298 mm and 674–838 mm, respectively (Crins *et al.* 2009). Their forests are primarily mixed (deciduous and coniferous) and they are also both classified as well-drained, with all waterways eventually leading to Lake Superior (Crins *et al.* 2009).

Study ponds were fishless semi-permanent and permanent ponds in the Thunder Bay region. These ponds could have been formed by man-made activities (i.e. ditches, trenches, or excavated lands), beavers, or natural seasonal flooding. Ponds ranged from 48 º to 49.6 º latitude. Surface area ranged from 33.5 m^2 to 3740.7 m^2, canopy cover ranged from 12 % to 68 %, and spring (May) depth ranged from 30 cm to 100 cm, whereas late summer (August) depth ranged from 14 cm to 92 cm. All sites were possible breeding sites for *L. sylvaticus*, *D. versicolor*, and Agabini beetles and were near forested land.

Table 2.1 Study Pond physical characteristics. Ponds with an * were kept in the analysis. Depth measurements were taken in May and August, 2024. Canopy closure, perimeter, and area measurements were taken in August 2024.

Pond ID	Latitude	Longitude	Depth	Canopy Closure	Perimeter	Area
Devrd1	48.05588	-89.73008	80 cm, 86 cm	67.8 %	318.3 m	3117.0 m^2
Cedarsites	48.23453	-89.90860	89 cm, 64 cm	22.7 %	109.2 m	662.2 m^2
Adrianlakerdpond	48.45271	-89.80561	100 cm, 89.5 cm	12.4 %	199.9 m	1963.6 m^2
Sunshinecabin *	48.55647	-89.74841	83.5 cm, 16 cm	61.3 %	22.2 m	33.5 m^2
Block3 *	48.79389	-89.87875	75 cm, 35 cm	61.4 %	58.1 m	182.8 m^2
DRT4 *	48.99677	-89.96132	30 cm, 92 cm	23.7 %	265.9 m	3740.7 m^2
DRT15 *	49.18415	-89.90292	56.5 cm, 22 cm	15.5 %	37.6 m	53.9 m^2
DRT20 *	49.26201	-89.82332	68.5 cm, 29.5 cm	48.1 %	102.8 m	279.1 m^2
DRT32	49.42664	-89.61480	42.5 cm, 14 cm	39.8 %	75.1 m	246.8 m^2
HW811.1 *	49.48179	-89.61594	70 cm, 71.5 cm	53.1 %	133.2 m	992.7 m^2
HW811.3b	49.64802	-89.88254	52 cm, 21.5 cm	44.1 %	94.2 m	318.7 m^2

2.2 Study species

In the boreal region of northwestern Ontario (Thunder Bay District), there are eight frog species that may use fishless ponds for breeding: Spring Peepers (*Pseudacris crucifer,* Hylidae), Boreal Chorus Frogs (*Pseudacris maculata,* Hylidae), Wood Frogs (*Lithobates sylvaticus,* Ranidae), American Toads (*Anaxyrus americanus,* Bufonidae), Green Frogs (*Lithobates clamitans,* Ranidae), Eastern Gray Treefrogs (*Dryophytes versicolor,* Hylidae), Mink Frogs (*Lithobates septentrionalis,* Hylidae), and Northern Leopard Frogs (*Lithobates pipiens,* Ranidae) (Harding & Mifsud 2017). Early spring breeders include Spring Peepers, Boreal Chorus Frogs, and Wood Frogs; species breeding later in the spring/summer include Eastern Gray Treefrogs, American Toads, Green Frogs, Mink Frogs, and Northern Leopard frogs (Dodd 2023).

I focused on *Lithobates sylvaticus* and *Dryophytes versicolor*. *L. sylvaticus* generally start breeding in northwestern Ontario in early–mid April. Females lay 300–2000 eggs in a cluster, usually attached to floating vegetation, and eggs take 1–3 weeks to hatch, and larvae take an additional 6–12 weeks to metamorphosize into adults, depending on water temperature (Dodd 2023). *L. sylvaticus* tadpoles are mostly herbivorous but may resort to cannibalism when resources are depleted (Jefferson *et al.* 2014).

D. versicolor start breeding (predominantly) in fishless pools in northwestern Ontario in late May. Eggs are typically deposited within the first two weeks of calling, but oviposition has been seen in August in the southern parts of their range (Dodd 2023). Eggs take from 2–3 weeks to hatch, and larvae take an additional 40–60 days to

metamorphose, depending on environmental temperatures. *D. versicolor* tadpoles are herbivorous and feed on algae and detritus (Harding & Mifsud 2017).

Tadpoles are prey for vertebrates and invertebrates, including birds, snakes, larger frogs, dragonflies and damselflies, predaceous beetles, and giant water bugs (Dodd 2023; Hocking & Semlitsch 2008). Both *D. versicolor* and *L. sylvaticus* tadpoles exhibit developmental and behavioural changes in response to predators. Tadpoles grow deeper and longer tails and adopt a more dormant lifestyle in the presence of predators (Relyea 2024; Shaffery & Relyea 2016; Trembath & Anholt 2001), and *D. versicolor* tadpoles also develop bright red colouring and black spots on their tails to attract a predator's attention away from their body (Bragg 1957). Tadpoles are capable of behavioural thermoregulation, and since they are practically isothermal with their environments, they can take advantage of pond thermal stratification to maintain a preferred body temperature (Lutterschmidt & Hutchison 1997), though such opportunities may be limited if pools are thermally homogeneous (Beltran 2019).

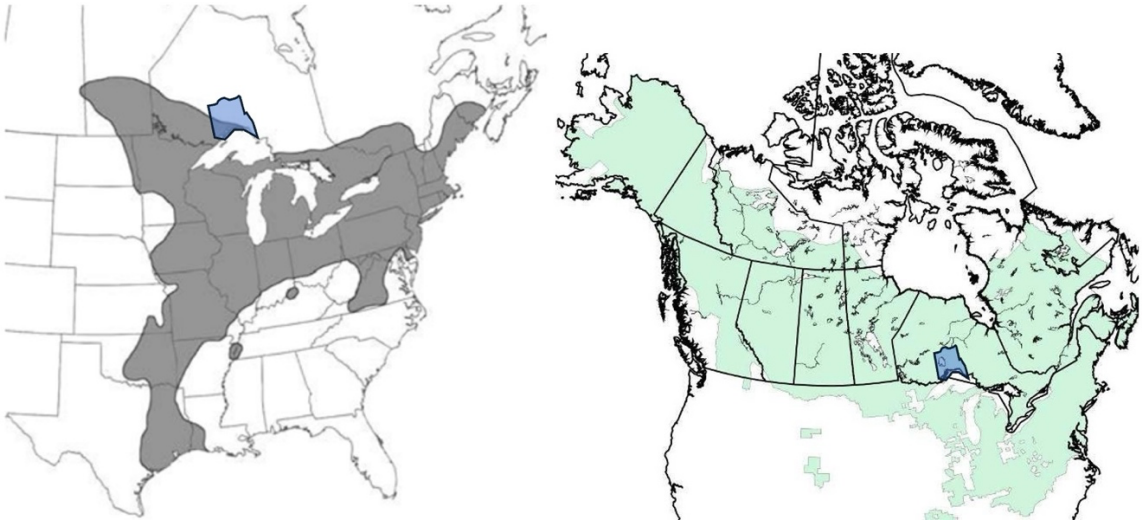

Figure 2.2. (Left) Distribution map of *Dryophytes versicolor* (Eastern Gray Treefrog) modified from Dodd (2023). The blue shaded region represents the Thunder Bay District, ON, Canada. (Right) Distribution map of *Lithobates sylvaticus* (Wood Frog) modified from Schock, 2009. The blue shaded region represents the Thunder Bay District, ON, Canada.

Invertebrate predators, specifically predaceous diving beetles (Dytiscidae), prey on many tadpole species. Both adult and larval forms of Dytiscidae are predaceous and may use different methods of prey capture, including ambush tactics and active chase (Culler *et al.* 2014). Within Dysticidae, the Agabini tribe consists of 9 genera. Animals used in my study could be from *Agabus* and/or *Ilybius*, which can only be reliably differentiated by taxonomic experts. Life cycle and breeding phenology vary across the Agabini tribe, however, any *Agabus spp.* collected in this study would likely have a Type 3 life cycle as described in Hilsenhoff (1993). In this type of life cycle, eggs overwinter in aquatic environments, and remnant adults (those that did not reproduce the previous summer) overwinter in terrestrial environments (Hilsenhoff 1993). Eggs hatch in early spring and larvae mature into adults by June, and most adults mate in the summer. In colder habitats, some adults may not emerge or mate until late summer, which pushes oviposition to the following spring instead of in their emergent summer (Hilsenhoff

1993). Any *Ilybius* spp. collected in this study would likely have a Type 1 life cycle from Hilsenhoff (1993). In this type of life cycle larvae overwinter in aquatic environments and mature into adults the following spring (Hilsenhoff 1993). Almost all adults mate by July and die shortly after. In colder habitats, it is possible for adults to overwinter in terrestrial habitats and mate the following spring (Hilsenhoff 1993). In the Thunder Bay region, adult Agabini phenologically overlap with *L. sylvaticus* tadpoles from at least mid-May and *D. versicolor* tadpoles from Late May – July (A. Algar, personal observation), making these species a likely prey choice. Agabini are widely distributed around North America (N.A.), most species are found in central N.A. (Manitoba–Ontario, southward to Tennessee and the Carolinas) (Hilsenhoff 1993). Dytiscidae hunting methods vary with ontogeny as larvae use powerful mandibles to grasp prey much larger than them, inject digestive enzymes into it, and suck the mixture back out through the mandible. Adults grasp prey and bite pieces off with their mouthparts, making them more gape-limited than larval dytiscids (Culler *et al.* 2014).

2.3 Pond and air temperature monitoring

I recorded water temperatures of 11 ponds from May 8, 2024, until September 18, 2024, along a 180 km S–N transect (Figure 2.1). Surface and substrate temperatures were recorded every hour using HOBO MX2201(Onset) data loggers (Figure 2.3). A data logger was secured in place at the bottom of each pond using a tall wooden stake; a surface logger was attached loosely to each stake so that it could rise and fall with water level. Summer (May–August) pond characteristics were also recorded for each pond including depth at temperature loggers (m), total pond surface area (m^2), pond perimeter (m), substrate type, canopy closure (%) at cardinal edges (north, east, south, west) and at

the pond centre, tree heights (m) at cardinal edges, and surrounding forest type. The 'track' function on a Garmin GPSMAP 67i was used to measure pond perimeter. Tracks, saved as FIIT files, were transformed into GPX files, uploaded into QGIS-LTR version 3.40.5-Bratislava (QGIS Development Team 2025) and pond perimeters and areas were calculated. Due to the accuracy of the GPS, which is 3 m, one site ('Sunshinecabin') was very difficult to accurately measure so I used Google Earth Pro version 7.3.6.10201 to get perimeter and area estimates for this site. For two other sites, 'DRT20' and 'HW811.3b', GPS tracks appeared inaccurate and difficult to interpret, perhaps because of their small size and surrounding, heavy, forest which could have caused satellite interference. These two sites were also too heavily forested and too small to be visible on Google Earth Pro; so, their GPS track-based measurements are less reliable than the others (Table 2.1). Canopy closure was measured using a convex spherical densitometer. Densiometers may overestimate canopy closure, relative to hemispherical photography) (Fiala *et al.* 2006). To account for this, I followed the corrections outlined by Strickler (1959) that restricts the sample area on the densiometer to reduce overlap of measurements. Tree heights were measured using a Nikon Forestry Pro II Laser Rangefinder. Pond perimeter and area, canopy cover, and tree heights were measured on August 12, 2024.

Air temperatures were recorded every hour from May until September 2024, at each study pond using HOBO MX2201 data loggers (Figure 2.4). Air temperature loggers were attached to nearby trees at each pond at ~1.3m. Each temperature logger was encased in a radiation shield, constructed following Holden *et al.* (2013), to reduce overestimation of air temperature by blocking the direct input of solar radiation on the logger.

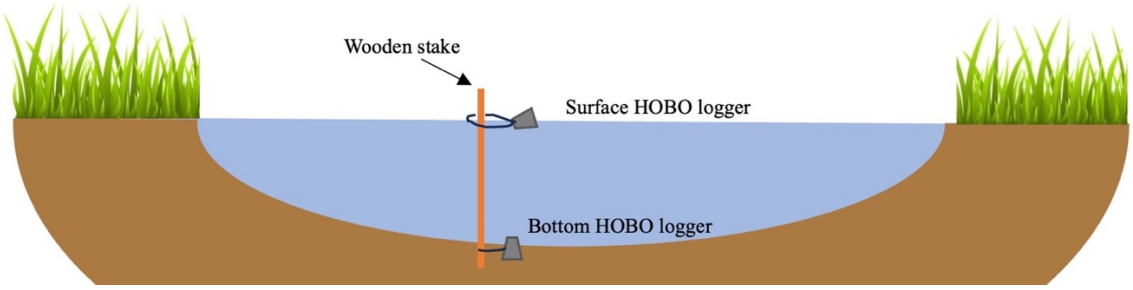

Figure 2.3. Equipment setup to record pond surface and bottom water temperatures in each study pond.

Figure 2.4. Setup to record air temperature at study ponds. The silver and white plastic rectangle is a radiation shield for the thermal logger (HOBO MX2201).

2.4 Animal collection

L. sylvaticus tadpoles were collected from a pond near Mapleward Road (48.407336°, -89.353178°) in Thunder Bay, Ontario, on May 15, 2024. Tadpoles were collected by agitating hatching egg masses until tadpoles swam out and into a net. Tadpoles were *circa* Gosner stage 21 at time of collection. Tadpoles were placed in a bucket of pond water and promptly transported to Lakehead University, counted, and placed into tanks in the Biology Aquatics Facility (BAF) for further development and

acclimation. Animals were placed into five 75 L tanks, with 25 individuals per tank, while the remaining individuals were put into a separate tank and used for feeding predators. Tanks were connected to a single recirculating filtration system and water quality parameters were checked daily. Agabini beetles were collected by hand that same day and placed into predator cages in the BAF tanks to provide predator-cues during tadpole development (Relyea 2024; Schoeppner & Relyea 2009). Tadpoles were fed algal wafers daily and predators were fed 5 mechanically euthanized tadpoles every 3 days. Tadpoles were held at 15 ºC for 7 days before experiments started.

D. versicolor eggs were collected from two amplectic pairs on the evening of June 1, 2024, captured in a breeding pond located at the Kamview Nordic Centre (48.330595°, -89.365565°). Each pair was transferred to a 5-gallon bucket filled with leaves, sticks, and pond water. Buckets were placed under tree cover (to avoid overheating after sun-up), left for 10 hours overnight and checked every two hours the following morning until oviposition finished. Adults were then released back into the breeding ponds and the buckets of eggs were brought to Lakehead University and added to rearing ponds, following Relyea (2018). Rearing ponds were plastic pools with a pond liner filled with 350 L of dechlorinated water, 10L of river water to introduce natural bacteria and microorganisms, 350g of leaf litter, and 15 g of Purina rabbit chow for food and covered with 50% shade cloth. Eggs were monitored daily for development and by June 10, 2024, 372 Gosner stage 20 tadpoles had been moved into the Lakehead University BAF for further development and acclimation. Animals were placed into five 75L tanks with 25 individuals per tank, as per *L. sylvaticus*. Agabini beetles were collected by hand that same day and placed into predator cages in the BAF tanks to give predator-cues during

tadpole development. Tadpoles were fed algal wafers daily and predators were fed 5 euthanized tadpoles every 3 days. Tadpoles were held at 15ºC for 7 days before experiments started.

Predaceous diving beetles (Family: Dytiscidae, Tribe Agabini) were collected from 3 different ponds located in the Thunder Bay city limits: Mapleward road (48.407336°, -89.353178°), Kamview Nordic Centre (48.330595°, -89.365565°, and Loch Lomond (48.295427°,-89.350891°). Bottle traps were deployed at edges of ponds and baited with raw meats on June 6, 2024. Traps were checked daily for 10 days and a total of 214 Agabini beetles were transported in individual containers to Lakehead University over this time. Agabini beetles were provided fresh dechlorinated water, a rock to hide under, and 10–15 bloodworms (Chironomidae) for food. Beetles were held in individual containers in large fridges set to 15 ºC for at least 5 days before being used in any experiments and they received fresh food and water every 3 days. The night before swim experiments, beetles were transported down and placed into individual cups in the tanks in the BAF to continue acclimating at 15ºC and be more accessible for experiments the following day.

2.5 Critical thermal maxima experiments (CT_{min} and CT_{max})

L. sylvaticus and *D. versicolor* tadpole critical thermal maxima were measured using established methods (Lutterschmidt & Hutchison 1997). For *L. sylvaticus*, tadpoles were Gosner stage 27/28 and for *D. versicolor*, stage 25. For each species, I measured the CT_{max} of 10 tadpoles, 2 from each tank to account for potential tank effects, then repeated this process for CT_{min}. Each individual was placed into an individual cup filled with 200mL of dechlorinated water which was placed in a 15°C water bath for 30 minutes

before heating or cooling began. Water was heated (or cooled) at a mean rate of 0.25 ± 0.12 ºC/min. During trials, tadpoles were gently prodded every 2 minutes with a pipette to check for responsiveness until the temperature reached 5 ºC from their anticipated thermal limit, at which point the tadpoles were prodded every 30 seconds. Heating/cooling continued until individuals did not respond to mechanical stimulation (Lutterschmidt & Hutchison 1997; Pintanel *et al.* 2022). I could not determine the CT_{min} for the *L. sylvaticus* tadpoles as I was only able to cool water to 4.4 °C and they showed no sign of being near their CT_{min} at this temperature. Once animals reached their critical thermal limits, they were immediately placed in 15 ºC water to recover. Animals were then euthanized using a neutral solution of Tricaine Methanesulfonate (TMS) and fixed in 10% formalin for morphological measurements.

I attempted to measure CT_{max} for Agabini beetles but could not identify consistent cues as to when an individual had reached its' thermal limit for 3 trial animals and thus, for ethical reasons, I did not continue with the thermal limit experiments for Agabini beetles.

2.6 Swim performance experiments

Swim speed experiments started the day after the critical thermal maxima experiments (Table 2.2). Again, to avoid confounding tank effects, two individual tadpoles were selected from each of the 5 experimental tanks (n = 10 for each temperature). Due to the small number of Agabini beetles captured and high mortality rates during acclimation, I tested only 5 beetles at each temperature. To measure swim speed, the same procedure was followed for tadpoles and beetles. Animals were placed individually into small cups filled with dechlorinated water and suspended in a water

bath. The water temperature was then either increased or decreased to the required swim speed test temperature at a mean rate of 0.25 ± 0.12 ºC/min. For *L. sylvaticus*, swim temperatures were 5 ºC, 10 ºC, 15 ºC, 20 ºC, 25 ºC, 29 ºC, 33 ºC, and 35 ºC. *D. versicolor* swim temperatures were 10 ºC, 15 ºC, 20 ºC, 25 ºC, 29 ºC, 31 ºC, 33 ºC, and 35 ºC. Beetle swim temperatures were 6.4 ºC, 10 ºC, 15 ºC, 20 ºC, 25 ºC, 29 ºC, 31 ºC, 33 ºC, and 35 ºC. 6.4 ºC was chosen as our lowest temperature for the Agabini beetles because this was the laboratory determined CT_{min} for *D. versicolor* and I wanted to better compare their performance at this temperature since we could not determine the CT_{min} or CT_{max} for the beetles. Due to time limitations because of the rate at which water could be heated and cooled, it was not feasible to randomize the treatment order, so the 4 coldest temperatures were measured on day 1 and the 4 warmest on day 2. Treatment order is unlikely to bias my results as independent sets of tadpoles were used for each temperature and developmental changes across 24 hours at 15 °C were expected to be slight. After the water bath reached the target temperature, animals were held in the bath for 30 minutes. After 30 minutes, each animal was placed in a 50 cm swim track filled with dechlorinated water at the target temperature. Animals were prodded gently with a pipette to initiate 3 different swim events. All swims were recorded using a GoPro Hero 11 in linear mode at 4K resolution and at 120 frames per second. After swimming, animals were immediately moved to a recovery cup filled with 15 ºC water. Animals were then euthanized and fixed in 10% formalin (tadpoles) or placed in 70% ethanol (beetles).

Table 2.2 Dates and timing of experiments and estimated Gosner stage (for tadpoles) at time of experiment.

Organism	Experiment type	Date	Gosner Stage
L. sylvaticus	CT_{min}	May 23, 2024 (morning)	26
	CT_{max}	May 23, 2024 (afternoon)	26
	Swim speed (Temperatures: 5ºC, 10ºC, 15ºC, and 20ºC)	May 24, 2024	27
	Swim speed (Temperatures: 25ºC, 29ºC, 33ºC, and 35ºC)	May 25, 2024	28
D. versicolor	CT_{min}	June 17, 2024 (morning)	24
	CT_{max}	June 17, 2024 (afternoon)	24
	Swim speed (Temperatures: 10ºC, 15ºC, 20ºC, 25ºC, and 29ºC)	June 18, 2024	25
	Swim speed (Temperatures: 31ºC, 33ºC, and 35ºC)	June 19, 2024	25
Agabini Beetles	CT_{min}	N/A	N/A
	CT_{max}	N/A	N/A
	Swim speed (Temperatures: 6.4ºC, 10ºC, 15ºC, 20ºC, and 25ºC)	June 25, 2024	N/A
	Swim speed (Temperatures: 29ºC, 31ºC, 33ºC, and 35ºC)	June 26, 2024	N/A

2.7 Swim speed analysis

I extracted maximum swim speed for each individual using the software Tracker (version 6.2.0; Brown *et al.* 2025). I analyzed the first 5 seconds of each swim event. Because tadpole heads move laterally when they swim, I measured swim speed by recording the distance travelled, in Tracker, every 0.1 seconds to better capture forward movement. Swim videos were analyzed blind (i.e. I did not know which treatment/temperature I was analyzing at the time) by randomizing file names to avoid unconscious bias. In total, I analyzed 198 videos (77 *L. sylvaticus* tadpoles, 78 *D. versicolor* tadpoles, and 43 Agabini beetles). Some swim trials were omitted: the camera overheated and did not record 2 of the *L. sylvaticus* swims; 1 of the *D. versicolor* tadpoles was injured and could not swim well. Also 2 of the beetles died overnight and thus sample sizes for temperatures 10 ºC and 25 ºC were 4 instead of 5.

2.8 Morphological measurements

I took photographs of tadpoles and beetles using an Olympus Tough TG-6 4K camera and a Leica EZ 4W A microscope. Body length (BL), tail length (TL), and tail height (TH) and body width (BW) were measured from the photos using ImageJ version 1.53 (Schneider *et al.* 2012). Tadpole total length was also calculated as the sum of body length (BL) and tail length (TL). Tadpoles were staged in water to allow a natural position of the tail fin for accurate tail height measurements as well as on their sides under the microscope for capturing the full body. Beetles were staged on their dorsal and ventral surfaces to provide detailed images of appendages (Figure 2.5).

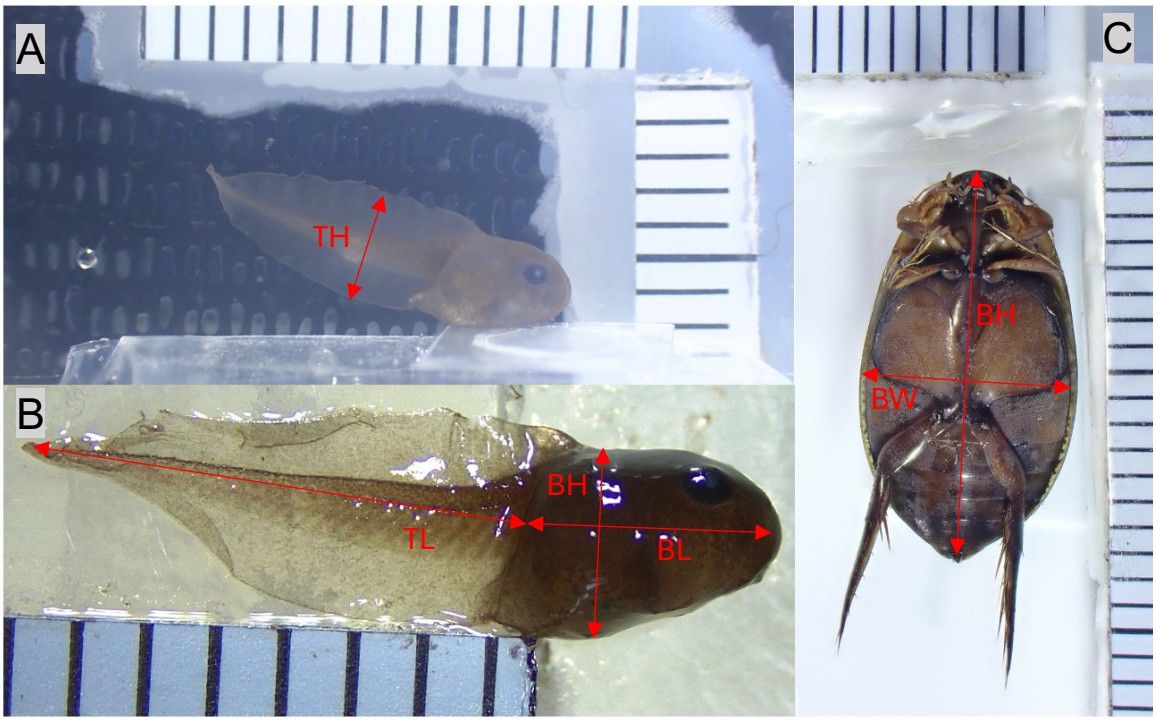

Figure 2.5. (A) *L. sylvaticus* tadpole positioned in water to show full tail fin. (B) *L. sylvaticus* tadpole positioned flat under microscope for length measurement. (C) Dytiscidae diving beetle showing ventral surface for body length and width. All measurements taken are shown with red lines. TH = tail fine height, TL = Tail length, BL = Body length, BW = Body width.

2.9 Fitting thermal performance curves

I used model averaging to obtain a thermal performance curve for each species. Thermal performance curves were fit using the rTPC package (version 1.0.4; Padfield & O'Sullivan 2023) in R 4.5.1 (R Core Team 2025). I fit 17 models to the *L. sylvaticus* data (Table 2.3). then used corrected Akaike weights to obtain a weighted average curve across all models. I repeated this using 16 models for *D. versicolor* and 15 models for Agabini beetles (Table 2.3). I used bootstrapping to estimate 95% confidence intervals for each curve. To do this, I randomly sampled, with replacement, the data in each temperature treatment and then refit the models to this data, calculated AICcs, found the weighted average model, and repeated this for 250 iterations. I then calculated the minimum and maximum predicted value from 237 of the 250 iterations (95%) at 0.1ºC increments to outline the 95% confidence intervals.

Table 2.3. Available models (at the time of my analysis) in the rTPC package (Padfield & O'Sullivan 2023). A checkmark marks models used for different organisms. Models without checkmarks were not used for those organisms.

Model name	Formula	Used for			Reason for exclusion:
		D. versicolor	*L. sylvaticus*	Agabini beetles	
"beta_2012"	$rate = \frac{a(\frac{temp - b + \frac{c(d-1)}{d+e-2}}{c})^{d-1} \cdot (1 - \frac{temp - b + \frac{c(d-1)}{d+e-2}}{c})^{e-1}}{(\frac{d-1}{d+e-2})^{d-1} \cdot (\frac{e-1}{d+e-2})^{e-1}}$	✓	✓	✓	
"boatman_2017"	$rate = r_{max} \cdot (sin(\pi(\frac{temp - t_{min}}{t_{max} - t_{min}})^a))^b$	✓	✓		Curve shape changes with every attempt, unreliable and not repeatable (beetles)
"briere2_1999"	$rate = a \cdot temp \cdot (temp - t_{min}) \cdot (t_{max} - temp)^{\frac{1}{b}}$	✓	✓	✓	
"delong_2017"	$rate = c \cdot exp\frac{-(e_a - (e_f(1 - \frac{temp + 273.15}{t_m})) + e_{hc} \cdot ((temp + 273.15) - t_m - (temp + 273.15) \cdot ln(\frac{temp + 273.15}{t_m})))}{k \cdot (temp + 273.15)}$				Starting values could not be calculated
"deutsch_2008"	$\text{if } temp < t_{opt}: rate = r_{max} \cdot exp^{-(\frac{temp - t_{opt}}{2a})^2}$ $\text{if } temp > t_{opt}: rate = r_{max} \cdot (1 - (\frac{temp - t_{opt}}{t_{opt} - ct_{max}})^2)$	✓	✓	✓	
"flinn_1991"	$rate = \frac{1}{1 + a + b \cdot temp + c \cdot temp^2}$			✓	Curve shape changes with every attempt, unreliable and not repeatable (tadpoles)
"gaussian_1987"	$rate = r_{max} \cdot exp^{(-0.5(\frac{\lvert temp - t_{opt} \rvert}{a})^2)}$				Will only fit symmetrical curves
"hinshelwood_1947"	$rate = a \cdot exp^{\frac{-e}{k \cdot (temp + 273.15)}} - b \cdot exp^{\frac{-e_h}{k \cdot (temp + 273.15)}}$				Curve shape changes with every attempt, unreliable and not repeatable
"joehnk_2008"	$rate = r_{max}(1 + a((b^{temp - t_{opt}} - 1) - \frac{ln(b)}{ln(c)}(c^{temp - t_{opt}} - 1)))$	✓	✓	✓	
"johnsonlewin_1946"	$rate = \frac{r_0 \cdot exp^{\frac{-e}{k \cdot (temp + 273.15)}}}{1 + exp^{-\frac{e_h - (\frac{e_h}{(t_{opt} + 273.15)} + k \cdot ln(\frac{e}{e_h - e})) \cdot (temp + 273.15)}{k \cdot (temp + 273.15)}}}$	✓	✓		Starting values could not be calculated (beetles)
"kamykowski_1985"	$rate = a \cdot (1 - exp^{-b \cdot (temp - t_{min})}) \cdot (1 - exp^{-c \cdot (t_{max} - temp)})$	✓	✓	✓	
"lactin2_1995"	$rate == exp^{a \cdot temp} - exp^{a \cdot t_{max} - (\frac{t_{max} - temp}{\delta_t})} + b$	✓	✓	✓	
"lrf_1991"	$rate = rmax \cdot (1 - \frac{(temp - topt)^2)}{(temp - topt)^2 + temp \cdot (tmax + tmin - temp) - tmax \cdot tmin}$		✓	✓	Curve shape changes with every attempt, unreliable and not repeatable (*D. versicolor*)
"modifiedgaussian_2006"	$rate = r_{max} \cdot \exp\left[-0.5(\frac{\lvert temp - t_{opt} \rvert}{a})^b\right]$				Does not fit a smooth curve, only fits 2 mirrored exponential lines
"oneill_1972"	$rate = r_{max} \cdot (\frac{ct_{max} - temp}{ct_{max} - t_{opt}})^x \cdot exp^{x \frac{temp - t_{opt}}{ct_{max} - t_{opt}}}$ $where: x = \frac{w^2}{400} \cdot (1 + \sqrt{1 + \frac{40}{w}})^2$ $and: w = (q_{10} - 1) \cdot (ct_{max} - t_{opt})$	✓	✓	✓	
"pawar_2018"	$rate = \frac{r_{tref} \cdot exp^{\frac{-e}{k}(\frac{1}{temp + 273.15} - \frac{1}{t_{ref} + 273.15})}}{1 + (\frac{e}{eh - e}) \cdot exp^{\frac{e_h}{k}(\frac{1}{t_{opt} + 273.15} - \frac{1}{temp + 273.15})}}$	✓	✓		Starting values could not be calculated (beetles)
"quadratic_2008"	$rate = a + b \cdot temp + c \cdot temp^2$				Will only fit symmetrical curves
"ratkowsky_1983"	$rate = (a \cdot (temp - t_{min}))^2 \cdot (1 - exp(b \cdot (temp - t_{max})))^2$	✓	✓	✓	
"rezende_2019"	$\text{if } temp < b: rate = a \cdot 10^{\frac{\log_{10}(q_{10})}{(\frac{10}{temp})}}$ $\text{if } temp > b: rate = a \cdot 10^{\frac{\log_{10}(q_{10})}{(\frac{10}{temp})}} \cdot (1 - c \cdot (b - temp)^2)$	✓	✓	✓	
"sharpeschoolfull_1981"	$rate = \frac{r_{tref} \cdot exp^{\frac{-e}{k}(\frac{1}{temp + 273.15} - \frac{1}{t_{ref} + 273.15})}}{1 + exp^{\frac{e_l}{k}(\frac{1}{t_l} - \frac{1}{temp + 273.15})} + exp^{\frac{e_h}{k}(\frac{1}{t_h} - \frac{1}{temp + 273.15})}}$				Not all parameters could be estimate from my data
"sharpeschoolhigh_1981"	$rate = \frac{r_{tref} \cdot exp^{\frac{-e}{k}(\frac{1}{temp + 273.15} - \frac{1}{t_{ref} + 273.15})}}{1 + exp^{\frac{e_h}{k}(\frac{1}{t_h} - \frac{1}{temp + 273.15})}}$	✓	✓		Starting values could not be calculated (beetles)
"sharpeschoollow_1981"	$rate = \frac{r_{tref} \cdot exp^{\frac{-e}{k}(\frac{1}{temp + 273.15} - \frac{1}{t_{ref} + 273.15})}}{1 + exp^{\frac{e_l}{k}(\frac{1}{t_l} - \frac{1}{temp + 273.15})}}$				Not all parameters could be estimate from my data
"spain_1982"	$rate = r_0 \cdot exp^{a \cdot temp} \cdot (1 - b \cdot exp^{c \cdot temp})$	✓	✓	✓	
"thomas_2012"	$rate = a \cdot exp^{b \cdot temp}(1 - (\frac{temp - t_{ref}}{c/2})^2)$	✓	✓	✓	
"thomas_2017"	$rate = a \cdot exp^{b \cdot temp} - (c + d \cdot exp^{e \cdot temp})$			✓	Curve shape changes with every attempt, unreliable and not repeatable (tadpoles)
"weibull_1995"	$rate = a \cdot (\frac{c-1}{c})^{\frac{1-c}{c}}(\frac{temp - t_{opt}}{b} + (\frac{c-1}{c})^{\frac{1}{c}})^{c-1} exp^{-(\frac{temp - t_{opt}}{b} + (\frac{c-1}{c})^{\frac{1}{c}})^c} + \frac{c-1}{c}$	✓	✓	✓	

2.10 Comparing predator and prey thermal performance curves (TPCs)

I compared parameters of the predator (beetle) and prey (*L. sylvaticus* or *D. versicolor*) TPCs: thermal optima (T_{opt}), thermal breadth (T_{br}) and performance at warm (35 °C) and cold (6.4 °C for *L. sylvaticus*, 10 °C for *D. versicolor*) temperatures. To test if these differed significantly among predators and prey, I used randomization tests. For each predator-prey pair, I randomly assigned swim speed estimates at each temperature to predator or prey (maintaining sample sizes) and refit model-averaged TPCs. I then calculated TPC parameters from each randomized curve and computed the difference between predator and prey values. I repeated this process 1000 times to obtain a null distribution of expected differences between predator and prey for each parameter. I used this distribution to calculate a two-tailed P-value (following Ruxton & Neuhäuser 2013) for the observed difference from the real predator and prey curves. The model 'beta_2012' had to be removed from the randomizations of *L. sylvaticus* and Agabini beetles because reliable fits could not be obtained for most of the iterations. Similarly, the model 'rezende_2019' was removed from the *D. versicolor* and beetle randomizations.

2.11 Projecting future pond temperatures

There are no existing projections of pond temperatures under future climate change for my study region (or any other similar one for which I am aware). Thus, I estimated future pond temperatures using my field data on air and pond temperature and existing climate change projections. First, I determined the relationship between air temperature and pond surface temperature using daily data from June 2024 for six of the 11 study ponds along my transect. I excluded 4 ponds (Table 2.1) because of missing data loggers (e.g. through interference by moose). One additional pond (Table 2.1) was excluded

because it was too close to another and thus they fell within the same grid cell of the raster of future climate projections. I determined the relationship between surface water temperature and substrate water temperature for only 5 of the 11 sites; 1 additional site (DRT 15) was removed from this portion of the analysis because the substrate data logger was missing (potentially stolen by an animal). Prior to model fitting, I tested if daily pond surface temperature (mean, minimum and maximum) from June 1 to July 31 varied with latitude by fitting linear mixed effects models with latitude as a fixed effect and date as a random effect. I found a statistically detectable increase in pond surface temperature with latitude, but this relationship was very weak, explaining only 3% of the variance in pond temperature (Figure 2.6). I repeated the above with pond bottom temperature and found similar results (marginal $R^2 < 0.02$ in all cases; Figure 2.6).

The slight increase in water temperature with latitude could be due to pond depth and canopy closure. The 2 southern-most sites had a more closed canopy (61% closure) than the rest of the northern sites, and they were also deeper at the start of the season than the more northern sites (Table 2.1). This could have made these ponds colder than the more open, shallower, northern ponds. Also, 'Block 3' (latitude 48.8) was especially cold as it was very deep, had a very dense canopy, was full of vegetation, and did not dry up by the end of the season (suggesting ground water input); all leading to a colder temperature throughout the season (Table 2.1). The slight increase in temperature with latitude is highly likely to be due to the physical characteristics of my study sites instead of air temperature.

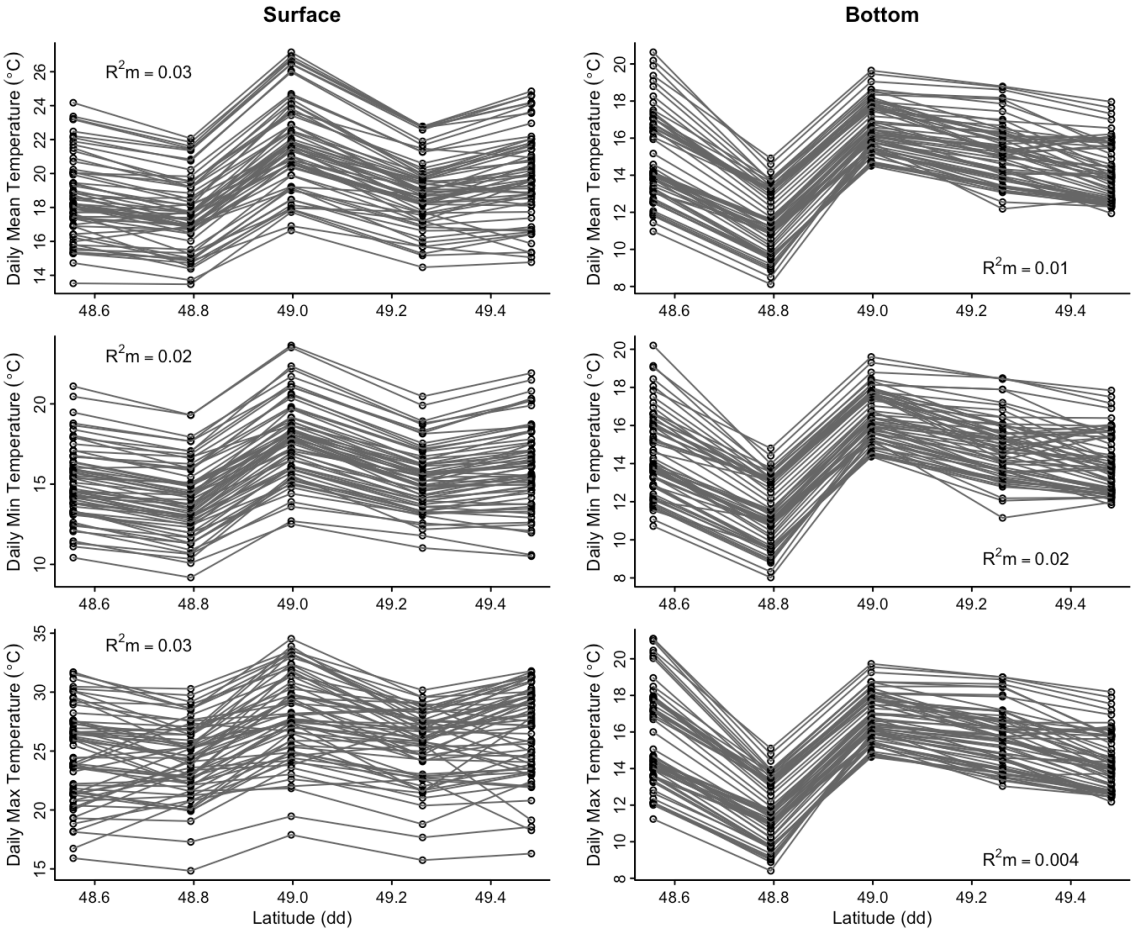

Figure 2.6. Relationship between daily surface water temperature (left) or bottom water temperature (right) with latitude in June across 5 study ponds. Lines connect measurements on the same date (June and July 2024). Marginal R^2 (R^2m) values give variance explained by latitude (fixed effects) based on a linear mixed effects model with latitude as a fixed effect and date as a random effect.

Since there was only a very weak relationship with latitude, I did not consider it further and treated my ponds as replicates to determine the relationship between pond surface temperature and air temperature during June. I averaged air and water temperature data across sites by date and then fit a gamma generalized linear model with a square-root link and daily average pond surface temperature as the response and daily average air temperature as the predictor. I fit additional models for daily minimum and daily maximum temperatures. I then fit a gamma generalized linear model with a logarithmic

link and daily average pond surface temperature as the response and daily average air temperature as the predictor. I repeated this for the daily minimum data but then fit a gamma generalized linear model with a square-root link and daily maximum pond surface temperature as the response and daily maximum air temperature as the predictor. I used different links for different data types to appropriately match the distribution of my response variables for each model. To test the assumptions of each model and ensure that they fit appropriately I used the R package 'DHARMa' to perform assumption tests (Hartig 2024).

I projected future pond temperatures using air temperatures from climate change scenarios and my gamma GLMs linking water and air temperature. I obtained projected daily summer (June and July) climate data (CanDCS-M6) from the Climate Scenarios Canada (Government of Canada, 2025b) for 2025–2100, for the nearest grid cells to each of my study sites. I considered four climate change scenarios: SSP1 (low emissions), SSP2 (moderate emissions), SSP3 (high emissions), SSP5 (extremely high emissions). I used my GLM for daily average surface temperature to predict pond surface temperature at each of my study pond locations for each scenario. I repeated this for daily minimum and maximum and for pond bottom temperatures. Climate data were organized in R using the package 'ncdf4' (Pierce 2025).

2.12 Quantifying relative predator-prey performance under climate change

To quantify the relative performance of predator and prey, I computed ΔV_T for my range of tested temperatures. To project how ΔV_T will respond to future climate change, I computed ΔV_T for the average June and July minimum, maximum and mean temperature for each year for each scenario. To test whether changes in ΔV were significant, I used t-

tests to compare ‘current’ values (2025–2035) to ‘future’ values (2085–2095). I did not use regression because of non-independence among climate among years.

3 Results

3.1 Impact of body size on swim speed

Significant growth occurred for *D. versicolor* between the swim speed experiments; day 2 tadpoles had longer bodies and taller tail fins than those on day 1, but no significant growth of their tail length or total length (Table 3.1). *L. sylvaticus* had significant growth between experimental days, with all measurements being significantly larger on day 2 (Table 3.1). However, there was no significant correlation between *L. sylvaticus* total length and swim speed ($p = 0.84$, $r = 0.023$) (Figure 3.1), nor was there a correlation between Agabini body length and swim speed ($p = 0.64$, $r = 0.074$) (Figure 3.1). There was a significant correlation between *D. versicolor* totally body length and swim speed ($p = 0.0052$, $r = 0.22$) (Figure 3.1), however, since there was no correlation between total length and treatment ($p = 0.74$, $r = 0.026$), I did not consider body size to influence the TPC results.

Table 3.1. Differences in morphological traits between testing days. Significant differences are bolded. 'Total length' is the sum of body length and tail length. Eastern Gray Treefrog (*D. versicolor*) tadpoles were tested on June 18, 2024 (n = 49) and June 19, 2024 (n = 29). Wood Frog (*L. sylvaticus*) tadpoles were tested on May 24, 2024 (n = 40) and May 25, 2024 (n = 40). Agabini Beetles were tested on June 25, 2024 (n = 23) and June 26, 2024 (n = 20).

Species	Trait	Test statistic	df	P-value
D. versicolor	Body length (BL)	t = -3.901	124.8	**<0.001**
	Tail length (TL)	t = 1.519	80.76	0.133
	Tail height (TH)	t = -2.239	98.73	**0.027**
	Total length	t = -0.236	89.18	0.81
L. sylvaticus	Body length (BL)	t = -6.575	138.9	**<0.001**
	Tail length (TL)	t = -3.931	131.9	**<0.001**
	Tail height (TH)	t = -6.660	141.7	**<0.001**
	Total length	t = -5.187	130.3	**<0.001**
Agabini beetles	Body length (BL)	t = 0.296	39.90	0.76
	Body width (BW)	t = 1.850	39.42	0.0718

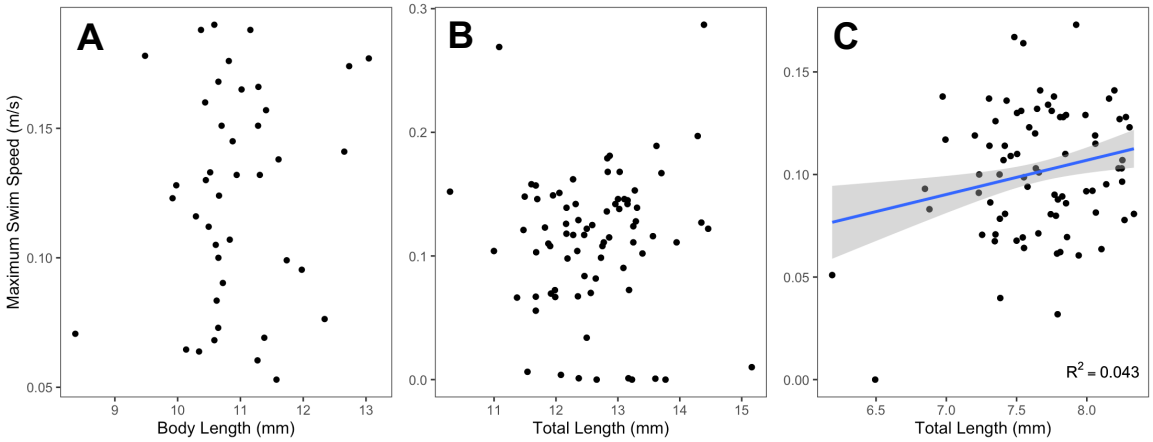

Figure 3.1. (A) correlation between Agabini adult beetle body length and their maximum swim speed (p = 0.64, r = 0.074). (B) correlation between *L. sylvaticus* tadpole body length (length of their tail + length of their body) and their maximum swim speed (p = 0.84, r = 0.023). (C) correlation between *D. versicolor* tadpole body length (length of their tail + length of their body) and their maximum swim speed (p = 0.05, r = 0.22).

3.2 Critical Thermal Limits (CT_{min} and CT_{max})

Table 3.2. Eastern Gray Treefrog tadpoles (*D. versicolor*), Wood Frog tadpoles (*L. sylvaticus*), and Agabini beetle thermal performance parameters: critical thermal minimum (CT_{min}), critical thermal maximum (CT_{max}), thermal optimum (T_{opt}), 80% thermal breadth ($T_{br(80\%)}$), i.e. the span of temperatures where performance is ≥80% of maximum, and maximum swim speed (swim speed at Topt). CTmin and CTmax were measured directly; T_{opt} and $T_{br(80\%)}$ were inferred from model-averaged thermal performance curves. Variation around the mean are standard deviations.

Species	CT_{min}	CT_{max}	T_{opt}	$T_{br(80\%)}$	Max speed
D. versicolor	6.4 ± 1.0 ºC	37.7 ± 2.2 ºC	24.2 ± 0.9 ºC	18.1 ± 0.9	0.122 ± 0.01 m/s
L. sylvaticus	-	37.2 ± 0.5 ºC	25.7 ± 3.2 ºC	19.1 ± 2.7	0.159 ± 0.02 m/s
Agabini	-	-	28.6 ± 1.6 ºC	13.5 ± 0.9	0.168 ± 0.01 m/s

3.3 Thermal performance curves

For *D. versicolor*, their performance was the lowest at the coldest tested temperature of 10 ºC and gradually increased to the T_{opt}, at 24.2 ºC, before gradually declining again until the warmest tested temperature of 35 ºC (Figure 3.2). The curve is relatively flat, with not much change in performance over the tested temperatures, and a wide $T_{br(80\%)}$ of 18.1 ± 0.9. Across all tested temperatures, *D. versicolor* swim speed ranged from 0.0725– 0.122 m/s.

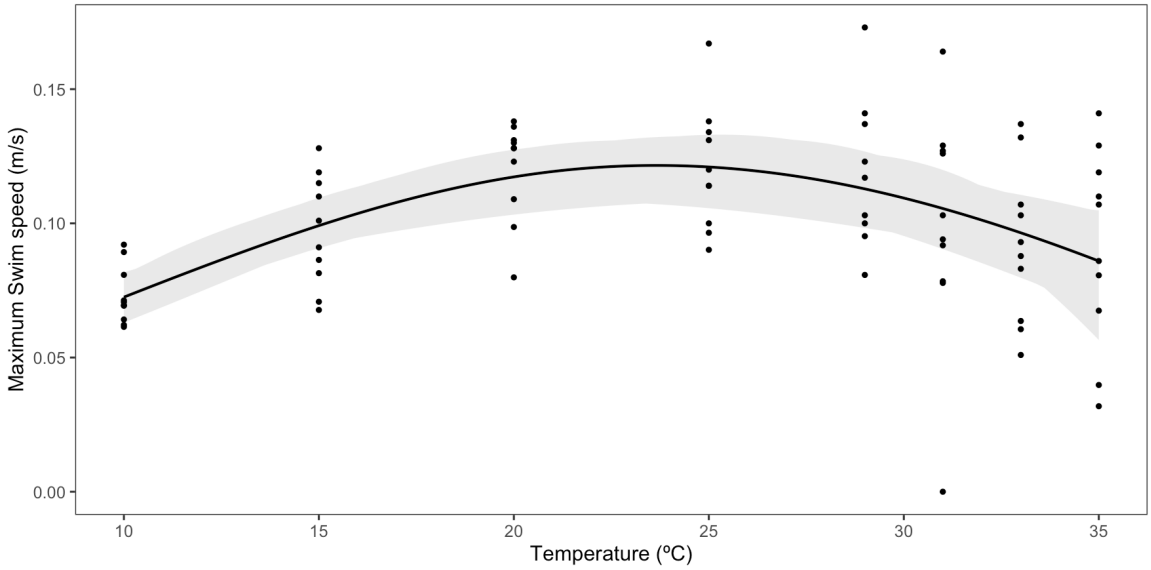

Figure 3.2. Eastern Gray Treefrog (*D. versicolor*) tadpole swim speed thermal performance curve (TPC). Black line dipicts the weighted mean curve composed of 16 different models from the "rTPC" package weighted by Akaike weights. Grey shaded area represents a boottsrapped 95% confidence interval made from refitting 244 iterations of randomized data (bootstrapping) and randomly selecting 95% of them (n =231).

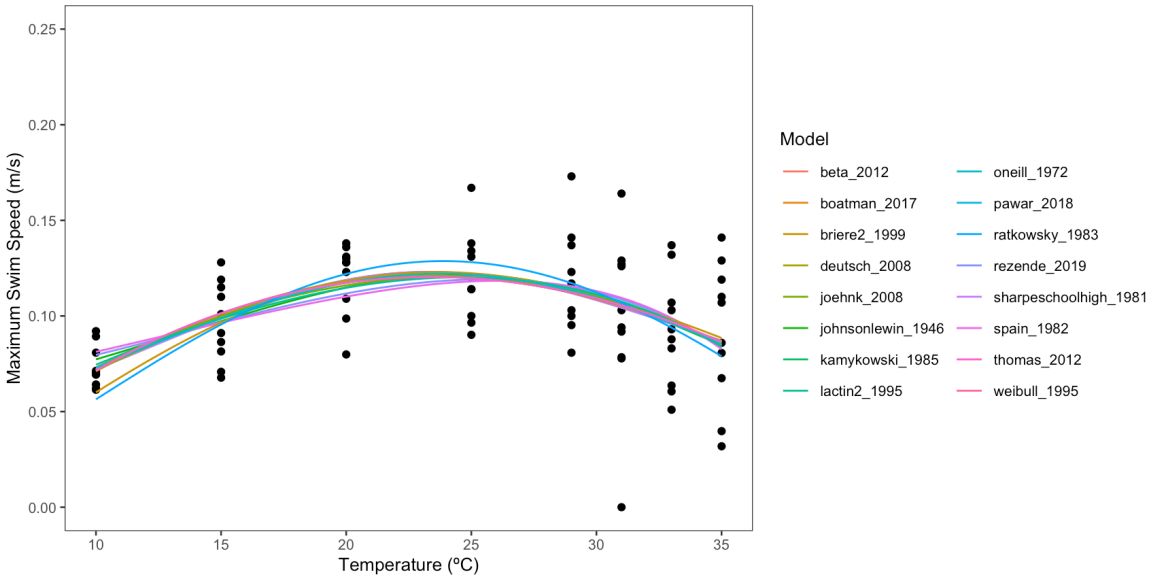

Figure 3.3. All 16 models fit to Eastern Gray Treefrog (*D. versicolor*) tadpole swim speed. Models used from the 'rTPC' package (version 1.0.4; Padfield &, O'Sullivan, 2023) in R 4.5.1 (R Core Team 2025).

Table 3.3. Estimators of model fits for *D. versicolor* swim speed from the 'rTPC' package (version 1.0.4; Padfield &, O'Sullivan, 2023) in R 4.5.1 (R Core Team 2025). Rank shows the best to worst fitting model based off AICc values. Models with the same rank number are equivalent.

Model name	AICc	ΔAICc	Akaike weight (w)	Rank
beta_2012	-333.32	2.56	0.03	8
boatman_2017	-333.08	2.80	0.03	10
briere2_1999	-333.25	2.62	0.03	9
deutsch_2008	-335.46	0.42	0.10	4
joehnk_2008	-332.65	3.23	0.02	13
johnsonlewin_1946	-335.04	0.84	0.08	6
kamykowski_1985	-332.85	3.02	0.03	12
lactin2_1995	-334.58	1.30	0.06	7
oneill_1972	-335.58	0.30	0.11	3
pawar_2018	-335.88	0.00	0.12	1
ratkowsky_1983	-329.97	5.91	0.01	15
rezende_2019	-332.95	2.93	0.03	11
sharpeschoolhigh_1981	-335.88	0.00	0.12	1
spain_1982	-331.81	4.07	0.02	14
thomas_2012	-335.20	0.68	0.09	5
weibull_1995	-335.61	0.27	0.11	2

For *L. sylvaticus*, their performance was the lowest at the warmest tested temperature of 35 ºC, since they were very close to their CT_{max}. Their performance was the second lowest at the coldest tested temperature of 5 ºC and gradually increased to the T_{opt}, 25.7 ºC, and stayed relatively high before sharply declining after 33–35 ºC (Figure 3.4). The curve is relatively flat throughout most tested temperatures but shows a sharp decline after 33 ºC and a wide $T_{br(80\%)}$ of 19.1 ± 2.7. Across all tested temperatures, *L. sylvaticus* swim speed ranged from 0.005– 0.159 m/s.

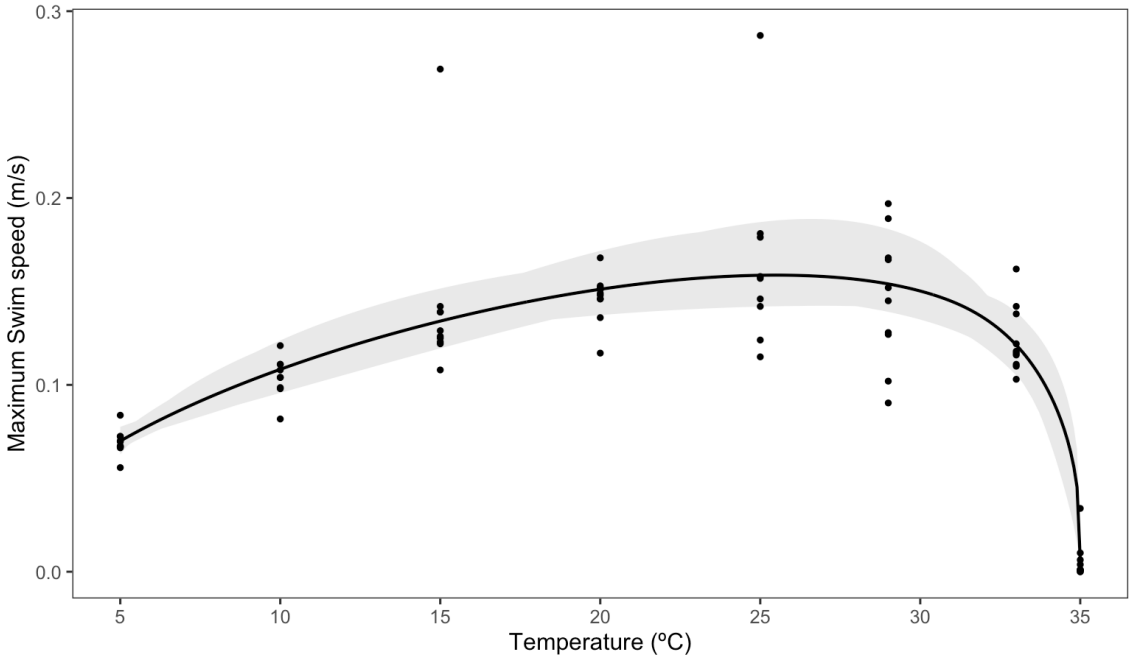

Figure 3.4. Wood Frog (*L. sylvaticus*) tadpole swim speed thermal performance curve (TPC). Black line dipicts the weighted mean curve composed of 17 different models from the "rTPC" package. Grey shaded area represents a bootstrapped 95% confidence interval made from refitting 250 iterations of randomized data (bootstrapping) and randomly selecting 95% of them (*n* =237).

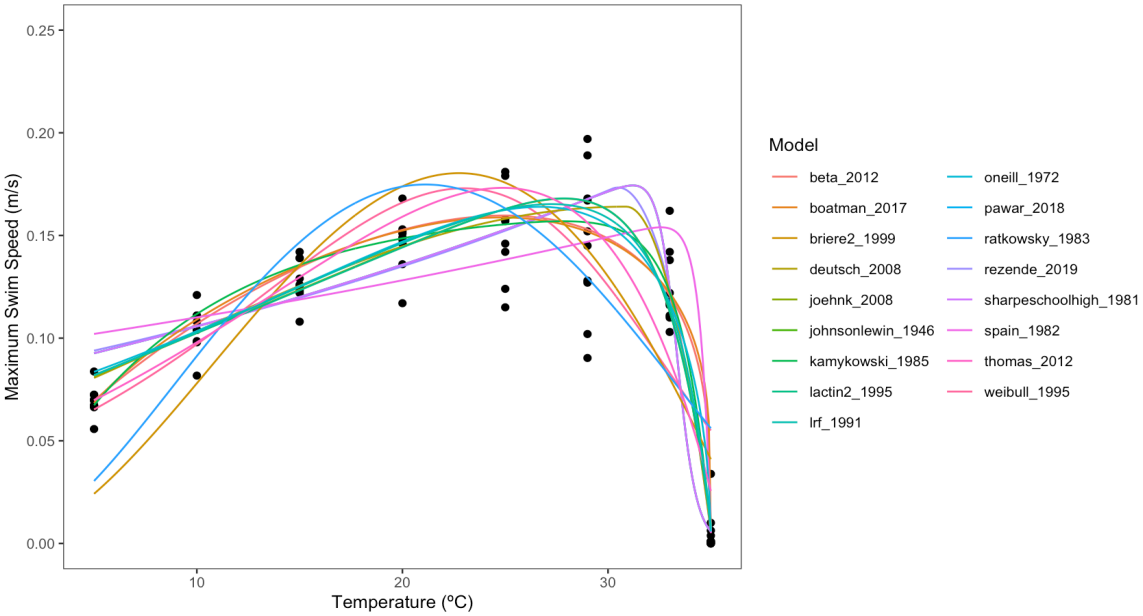

Figure 3.5. All 17 models fit to Wood Frog (*L. sylvaticus*) tadpole swim speed. Models used from the 'rTPC' package (version 1.0.4; Padfield &, O'Sullivan, 2023) in R 4.5.1 (R Core Team 2025).

Table 3.4. Estimators of model fits for *L. sylvaticus* swim speed from the 'rTPC' package (version 1.0.4; Padfield &, O'Sullivan, 2023) in R 4.5.1 (R Core Team 2025). Rank shows the best to worst fitting model based off AICc values. Models with the same rank number are equivalent.

Model name	AICc	ΔAICc	Akaike weight (w)	Rank
beta_2012	-325.88	0.12	0.35	2
boatman_2017	-325.99	0.00	0.37	1
briere2_1999	-270.36	55.63	3.10×10^{-13}	14
deutsch_2008	-321.11	4.88	0.033	5
joehnk_2008	-315.40	10.60	0.002	8
johnsonlewin_1946	-309.91	16.08	0.00012	9
kamykowski_1985	-324.48	1.52	0.175	3
lactin2_1995	-317.28	8.71	0.0048	7
lrf_1991	-320.40	5.60	0.023	6
oneill_1972	-321.35	4.65	0.037	4
pawar_2018	-309.91	16.08	0.00012	9
ratkowsky_1983	-268.10	57.90	1.00×10^{-13}	15
rezende_2019	-308.68	17.31	6.50×10^{-5}	10
sharpeschoolhigh_1981	-309.91	16.08	0.00012	9
spain_1982	-293.21	32.79	2.84×10^{-8}	12
thomas_2012	-306.35	19.64	2.03×10^{-5}	11
weibull_1995	-284.02	41.97	2.87×10^{-10}	13

For Agabini beetles, their performance was the lowest at the coldest tested temperature of 6.4 ºC and continuously increased to the T_{opt}, at 28.6 ºC, before sharply declining again until the warmest tested temperature of 35 ºC (Figure 3.6). The curve follows a characteristic shape and has a narrow $T_{br(80\%)}$ of 13.5 ± 0.9. Across all tested temperatures, Agabini swim speed ranged from 0.0658–0.168 m/s.

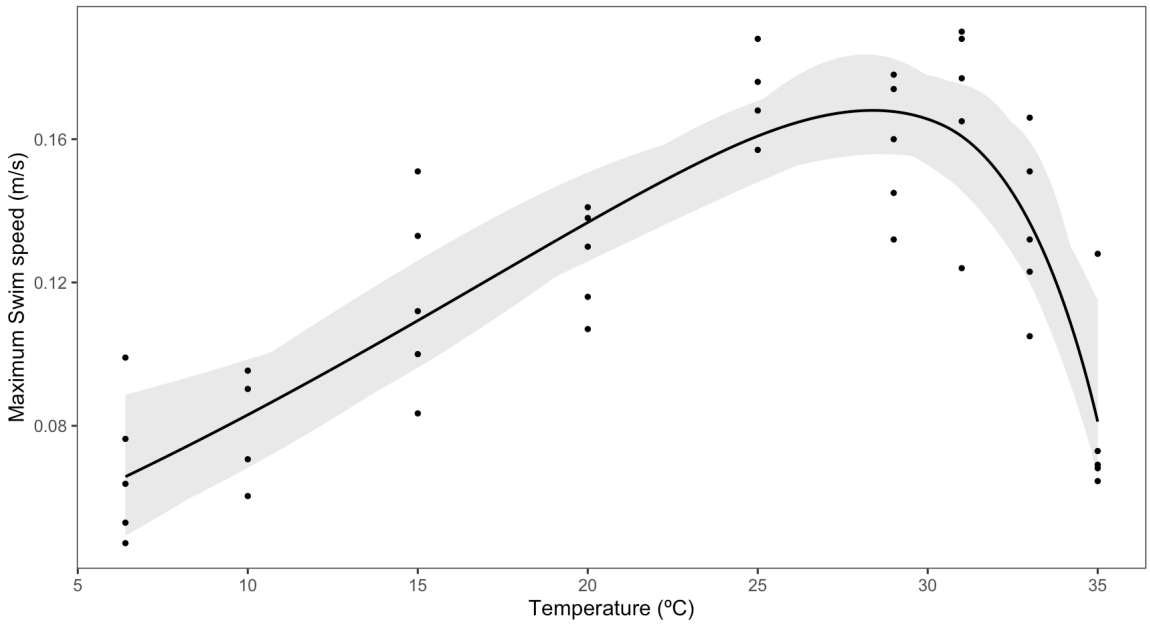

Figure 3.6. Agabini beetle (Family: Dytiscidae) swim speed thermal performance curve (TPC). Black line dipicts the weighted mean curve composed of 15 different models from the "rTPC" package. Grey shaded area represents a 95% confidence interval made from refitting 250 iterations of randomized data (bootstrapping) and randomly selecting 95% of them (n=237).

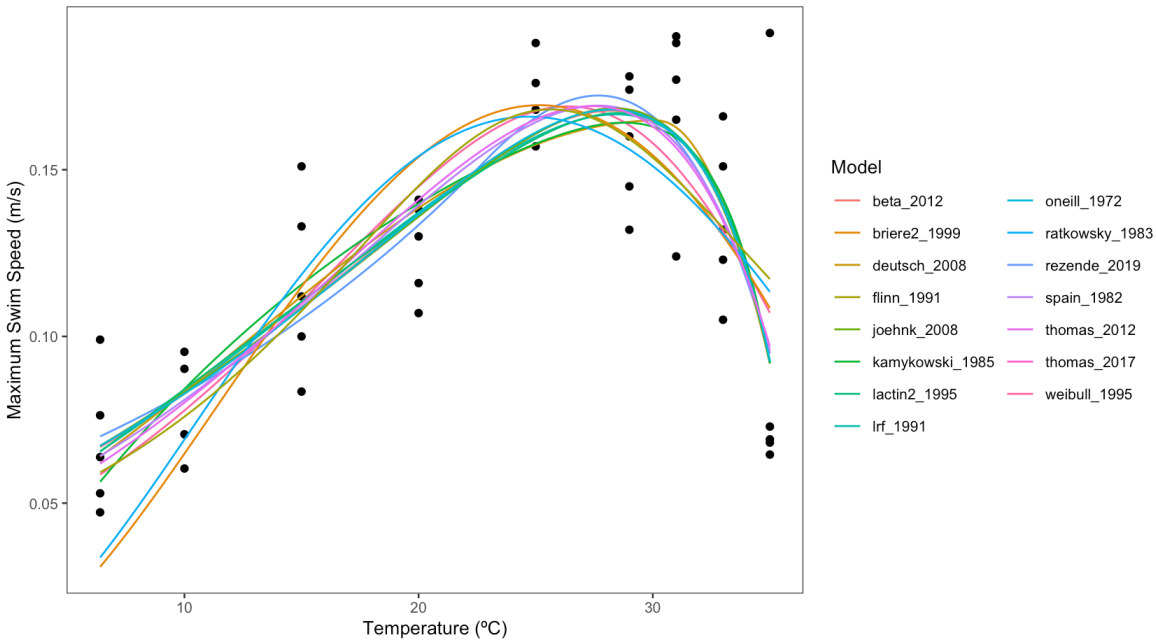

Figure 3.7. All 15 models fit to Agabini (Family: Dytiscidae) adult swim speed. Models used from the 'rTPC' package (version 1.0.4; Padfield &, O'Sullivan, 2023) in R 4.5.1 (R Core Team 2025).

Table 3.5. Estimators of model fits for adult Agabini (Family: Dytiscidae) swim speed from the 'rTPC' package (version 1.0.4; Padfield &, O'Sullivan, 2023) in R 4.5.1 (R Core Team 2025). Rank shows the best to worst fitting model based off AICc values. Models with the same rank number are equivalent.

Model name	AICc	ΔAICc	Akaike weight (w)	Rank
beta_2012	-179.61	2.73	0.035	8
briere2_1999	-165.99	16.35	3.86×10^{-5}	12
deutsch_2008	-182.24	0.11	0.13	3
flinn_1991	-176.97	5.37	0.0093	11
joehnk_2008	-179.66	2.68	0.036	7
kamykowski_1985	-178.03	4.31	0.016	9
lactin2_1995	-182.28	0.06	0.13	2
lrf_1991	-182.24	0.10	0.13	3
oneill_1972	-182.34	0.00	0.14	1
ratkowsky_1983	-165.81	16.53	3.52×10^{-5}	13
rezende_2019	-182.20	0.14	0.13	4
spain_1982	-181.91	0.43	0.11	5
thomas_2012	-181.38	0.96	0.085	6
thomas_2017	-179.66	2.68	0.036	7
weibull_1995	-178.00	4.34	0.016	10

3.4 Thermal Performance Curve comparisons

There were no significant differences found between *L. sylvaticus* tadpoles and Agabini beetles TPCs and there was major overlap between the two curves (Figure 3.8). However, for *D. versicolor* and Agabini beetles, the beetles had a clear performance advantage at warmer temperatures (Figure 3.9). Predator thermal optimum (T_{opt}) was 4.4 ºC greater than *D. versicolor* T_{opt} ($p = 0.025$) (Figure 3.10A) and was not significantly different from *L. sylvaticus* T_{opt} ($p = 0.163$) (Figure 3.11A). Predator thermal tolerance breadth ($T_{br(80\%)}$) was narrower than *D. versicolor* prey ($p = 0.040$) (Figure 3.10B) and not significantly different from *L. sylvaticus* prey ($p = 0.162$) (Figure 3.11B).

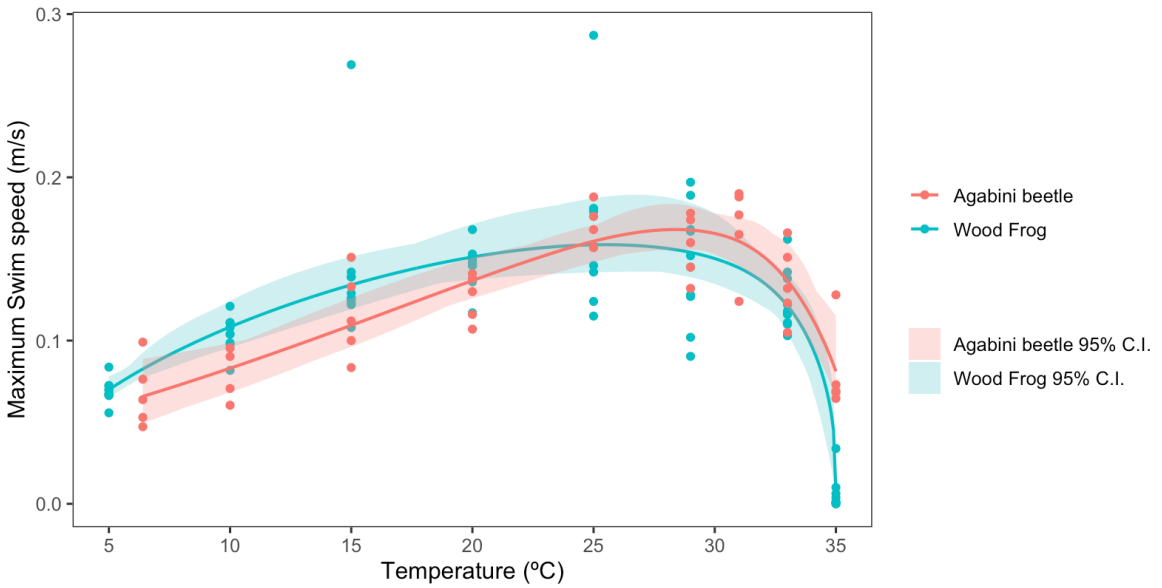

Figure 3.8. Wood Frog, *L. sylvaticus*, (blue) and Agabini beetle (red) thermal performance curves. Coloured lines show the respective curve for each organism, coloured shaded regions depict the 95% confidence intervals for each curve generated from bootstrapping.

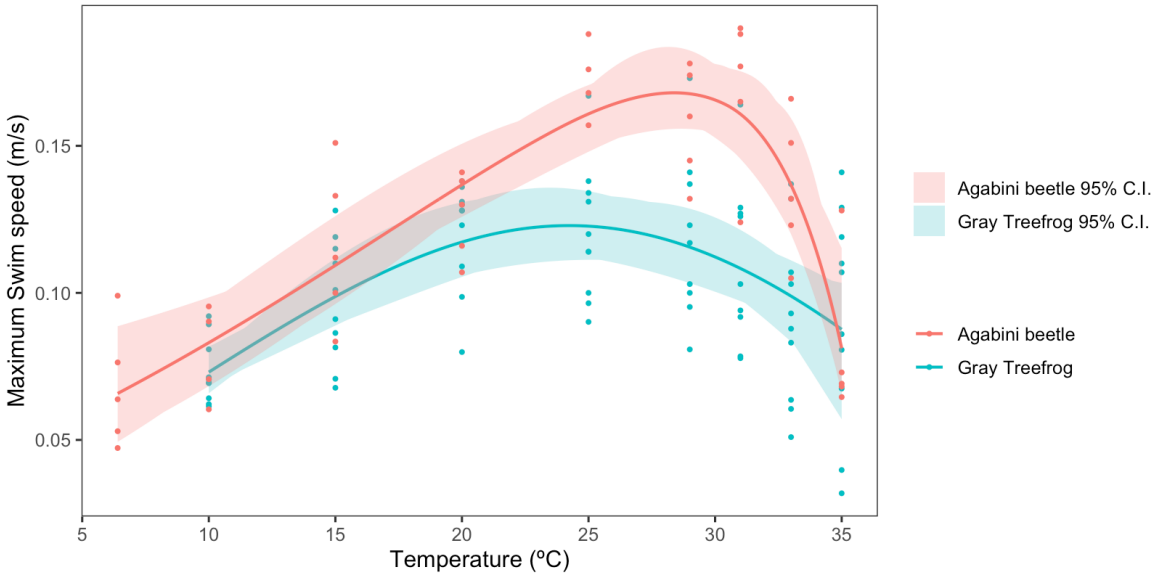

Figure 3.9. Eastern Gray Treefrog, *D. versicolor*, (blue) and Agabini beetle (red) thermal performance curves. Coloured lines show the respective curve for each organism, coloured shaded regions depict the 95% confidence intervals for each curve generated from bootstrapping.

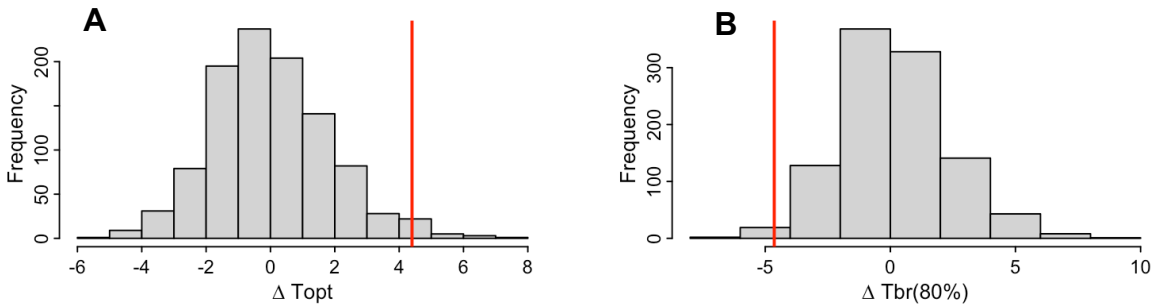

Figure 3.10. (A) ΔT_{opt}, Agabini beetle T_{opt} – *D. versicolor* T_{opt}, (red line) compared to the distribution of ΔT_{opt} values (histogram) from a null model analysis. (B) $\Delta T_{br(80\%)}$, Agabini beetle $T_{br(80\%)}$ – *D. versicolor* $T_{br(80\%)}$, (red line) compared to the distribution of $\Delta T_{br(80\%)}$ values (histogram) from a null model analysis. Results from 1038 randomizations of performance data. Solid lines show values that differed significantly from the null expectation (i.e. $p < 0.05$).

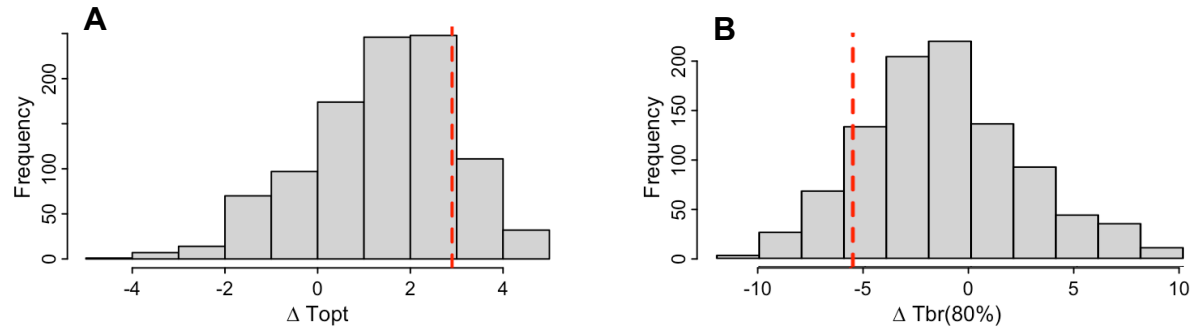

Figure 3.11. (A) ΔT_{opt}, Agabini beetle T_{opt} – *L. sylvaticus* T_{opt}, (red line) compared to the distribution of ΔT_{opt} values (histogram) from a null model analysis. (B) $\Delta T_{br(80\%)}$, Agabini beetle $T_{br(80\%)}$ – *L. sylvaticus* $T_{br(80\%)}$, (red line) compared to the distribution of $\Delta T_{br(80\%)}$ values (histogram) from a null model analysis. Results from 1038 randomizations of performance data. Solid lines show values that differed significantly from the null expectation (i.e. $p < 0.05$), striped lines did not differ from the null expectation (i.e. $p > 0.05$).

3.5 Pond temperatures in June and July 2024

Minimum, maximum, and average daily air temperature at my study sites was closely related to the corresponding daily surface water temperatures in June and July, 2024 (Figure 3.12). Surface water temperature was also fairly closely related to bottom water temperatures in June and July, 2024 (Figure 3.13).

Table 3.6. Range of daily average, minimum, and maximum air and pond temperatures across June and July 2024.

Daily Temp	Air temperature	Pond surface temperature	Pond bottom temperature
Average	10.5 – 24.1 ºC	14.7 – 24.0 ºC	12.0 – 18.1 ºC
Minimum	0.9 – 19.0 ºC	10.8 – 21.2 ºC	11.8 – 17.7 ºC
Maximum	12.9 – 31.2 ºC	16.1 – 31.4 ºC	12.4 – 18.5 ºC

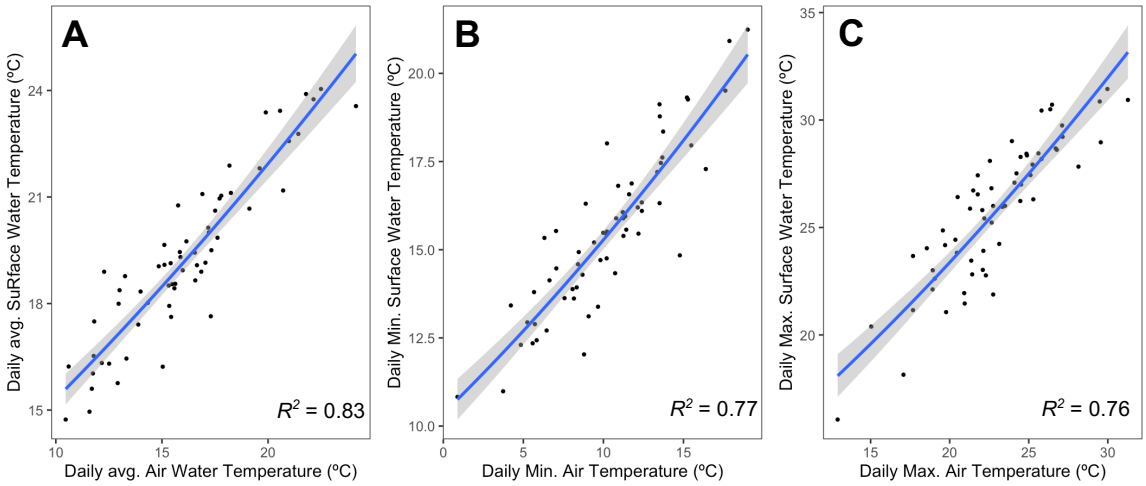

Figure 3.12. (A) Gamma family generalized linear model (GLM) with a square-root link of daily average air temperature and daily average surface water temperature in June & July, 2024. (B) Gamma family GLM with a square-root link of daily minimum air temperature and daily minimum surface water temperature in June & July, 2024. (C) Gamma family GLM with a square-root link of daily maximum air temperature and daily maximum surface water temperature in June & July, 2024. The blue line depicts the GLM and the grey shaded area shows the 95% confidence interval.

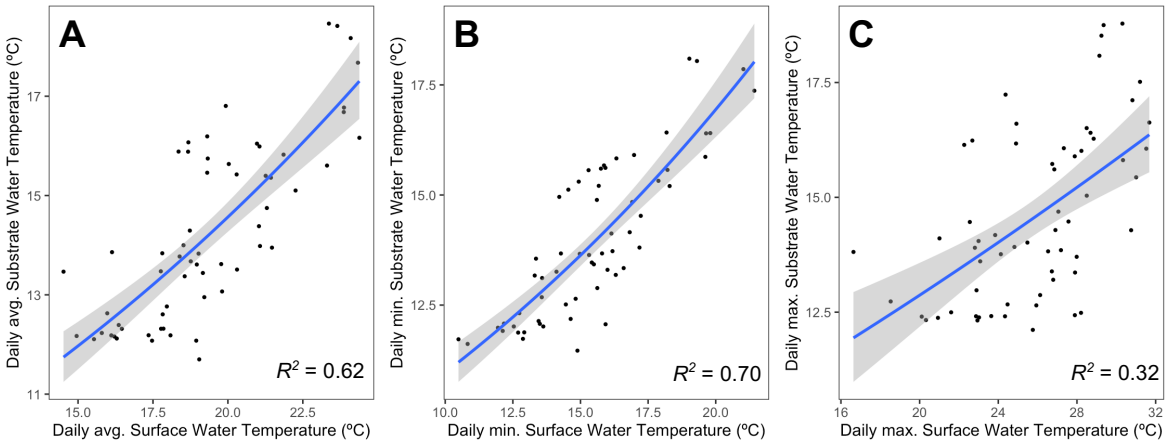

Figure 3.13. (A) Gamma family generalized linear model (GLM) with a log link of daily average surface water temperature and daily average bottom water temperature in June & July, 2024. (B) Gamma family GLM with a log link of daily minimum air temperature and daily minimum surface water temperature and daily minimum bottom water temperature in June & July, 2024. (C) Gamma family GLM with a square-root link of daily maximum surface water temperature and daily maximum bottom water temperature in June & July, 2024. The blue line depicts the GLM and the grey shaded area shows the 95% confidence interval.

Table 3.7. Gamma family generalized linear model (log or square-root links) equations for modelling environmental data from 2024. Gamma generalized linear model equations are back transformed to the response variable.

Model	Data	Model equation
glm(surface temp ~ air temp), Gamma (link = sqrt)	Daily avg	$T_{surface} = (3.142 + 0.077 * T_{air})^2$
glm(surface temp ~ air temp), Gamma (link = sqrt)	Daily min	$T_{surface} = (3.218 + 0.069 * T_{air})^2$
glm(surface temp ~ air temp), Gamma (link = sqrt)	Daily max	$T_{surface} = (3.196 + 0.082 * T_{air})^2$
glm(bottom temp ~ surface temp) Gamma (link = log)	Daily avg	$T_{bottom} = \exp(1.96 + 0.037 * T_{surface})$
glm(bottom temp ~ surface temp) Gamma (link = log)	Daily min	$T_{bottom} = \exp(2.03 + 0.040 * T_{surface})$
glm(bottom temp ~ surface temp) Gamma (link = sqrt)	Daily max	$T_{bottom} = \exp(2.23 + 0.018 * T_{surface})$

3.6 Predicted pond temperatures

Future pond surface water (Table 3.8) and bottom water (Table 3.9) temperatures were predicted to increase significantly through time for all scenarios (Figure 3.14 and Figure 3.15).

Table 3.8. Change in daily temperature estimates (daily average, daily minimum, and daily maximum) surface water temperature ($T_{surface}$) through time based off predicted climate data for 2025-2100. Climate scenarios are SSP1 = low emissions, SSP2 = moderate emissions, SSP3 = high emissions, and SSP5 = extremely high emissions. '2025' is the predicted daily surface water temperature from June & July 2025, '2100' is the predicted daily surface water temperature from June & July 2100. The slope represents the change in daily temperature per year. 'Corrected p-value' is the Bonferonni corrected p-values from t-tests comparing predicted temperatures between 'current' (2025-2035) to 'future' (2085-2095) June & July daily temperatures. Significant p-values are bolded.

Daily Temperature	Climate scenario	2025	2100	Slope	Corrected p-value
Average $T_{surface}$	SSP1	20.0 ºC	20.3 ºC	+0.004 ºC/year	**0.0168**
	SSP2	20.0 ºC	21.4 ºC	+0.019 ºC/year	**3.08×10^{-7}**
	SSP3	20.3 ºC	23.0 ºC	+0.036 ºC/year	**8.19×10^{-9}**
	SSP5	19.8 ºC	24.7 ºC	+0.065 ºC/year	**8.06×10^{-11}**
Minimum $T_{surface}$	SSP1	15.6 ºC	16.0 ºC	+0.005 ºC/year	**7.90×10^{-5}**
	SSP2	15.6 ºC	17.1 ºC	+0.02 ºC/year	**2.90×10^{-11}**
	SSP3	15.6 ºC	18.2 ºC	+0.035 ºC/year	**3.09×10^{-12}**
	SSP5	15.5 ºC	19.2 ºC	+0.049 ºC/year	**1.59×10^{-12}**
Maximum $T_{surface}$	SSP1	26.9 ºC	27.3 ºC	+0.005 ºC/year	**0.00572**
	SSP2	26.9 ºC	29.3 ºC	+0.32 ºC/year	**3.47×10^{-9}**
	SSP3	26.8 ºC	30.7 ºC	+0.052 ºC/year	**1.83×10^{-10}**
	SSP5	26.7 ºC	32.8 ºC	+0.081 ºC/year	**1.41×10^{-10}**

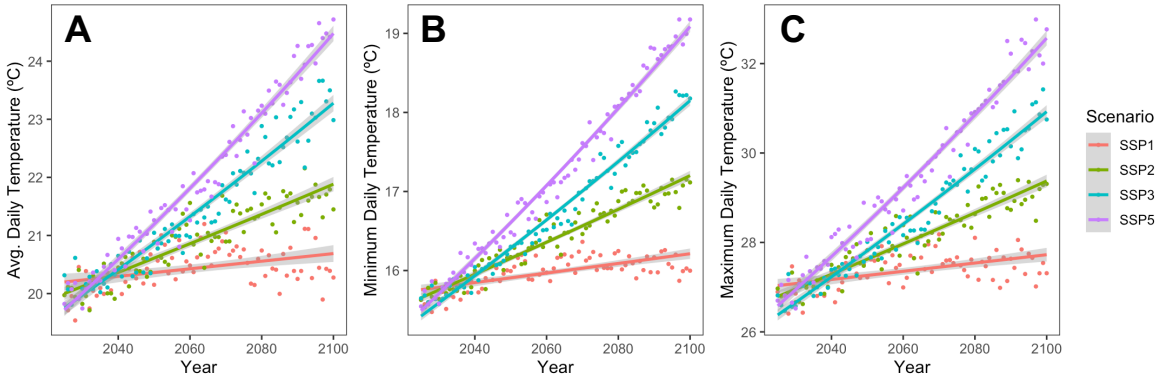

Figure 3.14. Projected change in June & July surface temperature ($T_{surface}$) of a representative pond for 2025-2100. (A) Mean daily temperature; (B) daily minimum temperature, (C) daily maximum temperature. Each coloured line represents a different climate scenario (SSP1 = low emissions, SSP2 = moderate emissions, SSP3 = high emissions, and SSP5 = extremely high emissions) and the grey shaded regions show the 95% confidence interval for each line.

Table 3.9. Change in daily temperature estimates (daily average, daily minimum, and daily maximum) bottom water temperature (T_{bottom}) through time based off predicted climate data for 2025-2100. Climate scenarios are SSP1 = low emissions, SSP2 = moderate emissions, SSP3 = high emissions, and SSP5 = extremely high emissions. '2025' is the predicted daily surface water temperature from June & July 2025, '2100' is the predicted daily surface water temperature from June & July 2100. The slope represents the change in daily temperature per year. 'Corrected p-value' is the Bonferonni corrected p-values from t-tests comparing predicted temperatures between 'current' (2025-2035) to 'future' (2085-2095) June & July daily temperatures. Significant p-values are bolded.

Daily Temperature	Climate scenario	2025	2100	Slope	Corrected p-value
Average T_{bottom}	SSP1	14.6 ºC	14.7 ºC	+0.0013 ºC/year	**0.0161**
	SSP2	14.6 ºC	15.5 ºC	+0.012 ºC/year	**3.6×10^{-7}**
	SSP3	14.8 ºC	16.4 ºC	+0.021 ºC/year	**1.11×10^{-8}**
	SSP5	14.5 ºC	17.6 ºC	+0.041 ºC/year	**1.48×10^{-10}**
Minimum T_{bottom}	SSP1	14.0 ºC	14.3 ºC	+0.004 ºC/year	**7.17×10^{-5}**
	SSP2	14.0 ºC	15.0 ºC	+0.013 ºC/year	**3.18×10^{-11}**
	SSP3	14.0 ºC	15.7 ºC	+0.023 ºC/year	**4.08×10^{-12}**
	SSP5	14.0 ºC	16.4 ºC	+0.032 ºC/year	**2.24×10^{-12}**
Maximum T_{bottom}	SSP1	14.9 ºC	15.6 ºC	+0.0093 ºC/year	**0.00528**
	SSP2	14.9 ºC	15.7 ºC	+0.011 ºC/year	**3.73×10^{-9}**
	SSP3	14.9 ºC	16.1 ºC	+0.016 ºC/year	**2.04×10^{-10}**
	SSP5	14.8 ºC	16.8 ºC	+0.027 ºC/year	**1.93×10^{-10}**

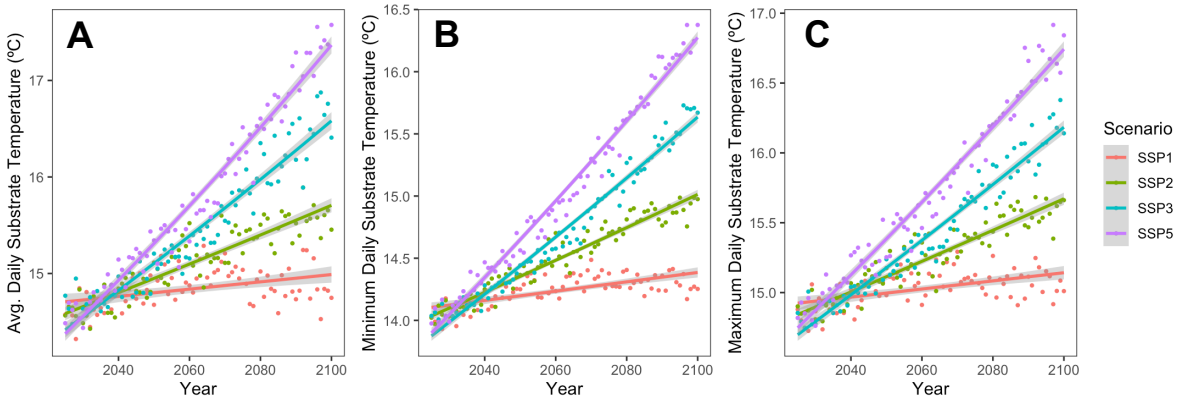

Figure 3.15. Projected change in June & July bottom temperature (T_{bottom}) of a representative pond for 2025-2100. (A) Mean daily temperature; (B) daily minimum temperature, (C) daily maximum temperature. Each coloured line represents a different climate scenario (SSP1 = low emissions, SSP2 = moderate emissions, SSP3 = high emissions, and SSP5 = extremely high emissions) and the grey shaded regions show the 95% confidence interval for each line.

3.7 Projected ΔV_T at the pond's surface

For daily average and minimum surface temperatures, ΔV_T significantly increased through time ($p < 0.001$) for all climate scenarios (Table 3.11). Increases in average ΔV_T between 2025 and 2100 varied from 0.0035 for SSP1 to 0.018 for SSP5, i.e. as expected, they were greatest for the highest emission scenarios (Table 3.10). Increases in minimum ΔV_T between 2025 and 2100 varied from 0.0004 for SSP1 to 0.0063 for SSP5, i.e. as expected, they were greatest for the highest emission scenarios (Table 3.10).

Daily maximum ΔV_T showed a different pattern and increased for SSP1-SSP5, with increases of 0.0014, 0.0064, and 0.0076 between 2025 and 2100 for each scenario, respectively (Table 3.10). However, for SSP5, ΔV_T peaked shortly after 2060 (Figure 3.16C), and then declined, resulting in a net change between 2025 and 2100 of -0.0048. This is the only scenario where ΔV_T was found to decrease by 2100 (Table 3.10).

Table 3.10. Change in ΔV_T at daily average, daily minimum, and daily maximum surface water temperatures from 2025-2100. Climate scenarios are SSP1 = low emissions, SSP2 = moderate emissions, SSP3 = high emissions, and SSP5 = extremely high emissions. '2025' is average ΔV from June & July 2025, '2100' is average ΔV from June & July 2100. The slope represents the change in ΔV_T per year. N/A is in place of maximum SSP5 because it was best fit by a quadratic model and does not have a single slope estimate.

Daily ΔV_T (surface)	Climate scenario	2025	2100	Slope
Average	SSP1	0.0195	0.0203	$+1.07 \times 10^{-5}$ ΔV_T/year
	SSP2	0.0195	0.0238	$+5.73 \times 10^{-5}$ ΔV_T/year
	SSP3	0.0203	0.0298	$+1.27 \times 10^{-4}$ ΔV_T/year
	SSP5	0.0189	0.0369	$+2.40 \times 10^{-4}$ ΔV_T/year
Minimum	SSP1	0.0112	0.0116	$+5.33 \times 10^{-6}$ ΔV_T/year
	SSP2	0.0112	0.0131	$+2.53 \times 10^{-5}$ ΔV_T/year
	SSP3	0.0112	0.0151	$+5.20 \times 10^{-5}$ ΔV_T/year
	SSP5	0.0111	0.0174	$+8.40 \times 10^{-5}$ ΔV_T/year
Maximum	SSP1	0.0459	0.0473	$+1.87 \times 10^{-5}$ ΔV_T/year
	SSP2	0.0463	0.0527	$+8.53 \times 10^{-5}$ ΔV_T/year
	SSP3	0.0455	0.0531	$+1.01 \times 10^{-4}$ ΔV_T/year
	SSP5	0.0451	0.0403	N/A

Table 3.11. Results from t-test between 'current' (2025-2035) and 'future' (2085-2095) June & July ΔV_T at the water's surface. 'Corrected p-value' is the Bonferonni corrected p-values from t-tests. Significant p-values are bolded.

Daily ΔV_T (surface)	Climate scenario	df	t-stat	Corrected p-value
Average	SSP1	10	-3.4094	**0.020**
	SSP2	10	-12.666	**5.26×10^{-7}**
	SSP3	10	-18.44	**1.42×10^{-8}**
	SSP5	10	-26.533	**4.00×10^{-10}**
Minimum	SSP1	10	-7.6133	**5.44×10^{-5}**
	SSP2	10	-35.681	**2.13×10^{-11}**
	SSP3	10	-31.672	**6.95×10^{-11}**
	SSP5	10	-40.167	**6.57×10^{-11}**
Maximum	SSP1	10	-3.8351	**0.0099**
	SSP2	10	-23.424	**1.37×10^{-9}**
	SSP3	10	-24.258	**9.69×10^{-10}**
	SSP5	10	-1.3878	0.0586

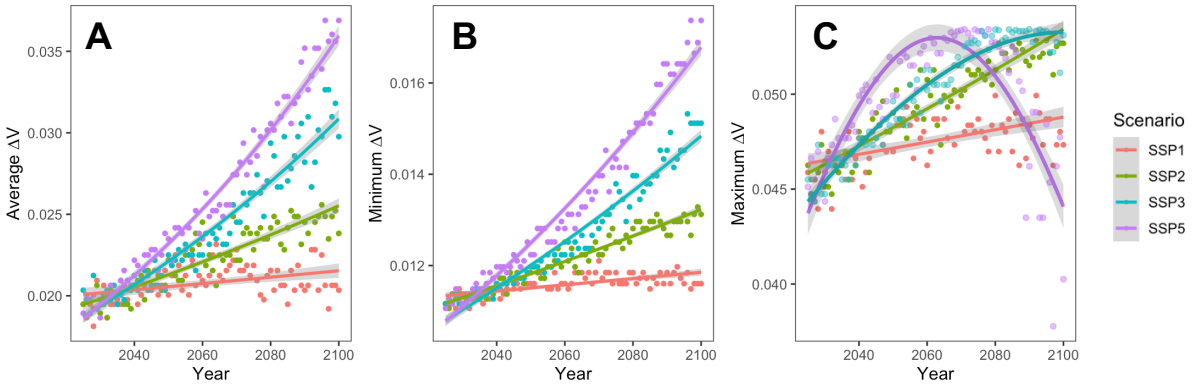

Figure 3.16. (A) corresponding ΔV_T values to predicted average daily June & July surface water temperatures from 2025–2100. (B) corresponding ΔV_T values to predicted minimum daily June & July surface water temperatures from 2025–2100. (C) corresponding ΔV_T values to predicted maximum daily June & July surface water temperatures from 2025–2100. Each coloured line represents a different climate scenario and the grey shaded regions show the 95% confidence interval for each line.

3.8 Projected ΔV_T at the bottom of the pond

For daily average, minimum, and maximum bottom temperatures, ΔV_T significantly increased through time ($p < 0.001$) for all climate scenarios (Table 3.13). Increases in average ΔV_T between 2025 and 2100 varied from 0.0001 for SSP1 to 0.0038 for SSP5, i.e. as expected, they were greatest for the highest emission scenarios (Table 3.12). Increases in minimum ΔV_T between 2025 and 2100 varied from 0.00015 for SSP1 to 0.00215 for SSP5, i.e. as expected, they were greatest for the highest emission scenarios (Table 3.12). Increases in maximum ΔV_T between 2025 and 2100 varied from 0.0001 for SSP1 to 0.0022 for SSP5, i.e. as expected, they were greatest for the highest emission scenarios (Table 3.12).

Table 3.12. Change in ΔV_T at daily average, daily minimum, and daily maximum bottom water temperatures from 2025-2100. Climate scenarios are SSP1 = low emissions, SSP2 = moderate emissions, SSP3 = high emissions, and SSP5 = extremely high emissions. '2025' is average ΔV from June & July 2025, '2100' is average ΔV_T from June & July 2100. The slope represents the change in ΔV_T per year.

Daily ΔV_T (bottom)	Climate scenario	2025	2100	Slope
Average	SSP1	0.0103	0.0104	1.33×10^{-6} ΔV_T/year
	SSP2	0.0103	0.0111	1.07×10^{-5} ΔV_T/year
	SSP3	0.0105	0.0121	2.13×10^{-5} ΔV_T/year
	SSP5	0.0102	0.0140	5.07×10^{-5} ΔV_T/year
Minimum	SSP1	0.00995	0.0101	2.00×10^{-6} ΔV_T/year
	SSP2	0.00995	0.0106	8.67×10^{-6} ΔV_T/year
	SSP3	0.00995	0.0113	1.80×10^{-5} ΔV_T/year
	SSP5	0.00995	0.0121	2.87×10^{-5} ΔV_T/year
Maximum	SSP1	0.0105	0.0106	1.33×10^{-6} ΔV_T/year
	SSP2	0.0105	0.0113	1.07×10^{-5} ΔV_T/year
	SSP3	0.0105	0.0117	1.60×10^{-5} ΔV_T/year
	SSP5	0.0105	0.0127	2.93×10^{-5} ΔV_T/year

Table 3.13. Results from t-test between 'current' (2025-2035) and 'future' (2085-2095) June & July ΔV_T at the water's surface. 'Corrected p-value' is the Bonferonni corrected p-values from t-tests. Significant p-values are bolded.

Daily temp. estimate	Climate scenario	df	t-stat	Corrected p-value
Average	SSP1	10	-3.4243	**0.0195**
	SSP2	10	-12.034	**8.54×10^{-7}**
	SSP3	10	-16.199	**5.00×10^{-8}**
	SSP5	10	-22.656	**1.9×10^{-9}**
Minimum	SSP1	10	-6.414	**2.31×10^{-4}**
	SSP2	10	-30.71	**9.43×10^{-11}**
	SSP3	10	-30.165	**1.13×10^{-10}**
	SSP5	10	-31.562	**7.19×10^{-11}**
Maximum	SSP1	10	-6.414	**0.00453**
	SSP2	10	-19.708	**7.43×10^{-9}**
	SSP3	10	-23.058	**1.6×10^{-9}**
	SSP5	10	-21.496	**3.18×10^{-9}**

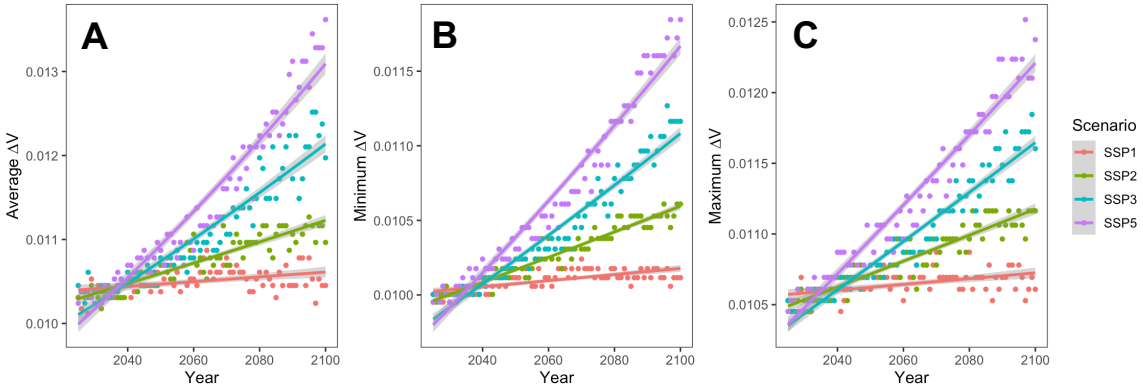

Figure 3.17. (A) corresponding ΔV_T values to predicted average daily June & July bottom water temperatures from 2025-2100. (B) corresponding ΔV_T values to predicted minimum daily June & July bottom water temperatures from 2025-2100. (C) corresponding ΔV_T values to predicted maximum daily June & July bottom water temperatures from 2025-2100. Each coloured line represents a different climate scenario and the grey shaded regions show the 95% confidence interval for each line.

4 Discussion

4.1 Summary

In this study, I compared thermal performance curves (TPCs) for predaceous Agabini beetles and two of their potential prey species: *D. versicolor* tadpoles, and *L. sylvaticus* tadpoles. Comparisons of these curves revealed that predators had a performance advantage at warmer temperatures over *D. versicolor* tadpoles but not *L. sylvaticus* tadpoles. Agabini beetles had a higher T_{opt} and narrower $T_{br(80\%)}$ than *D. versicolor*, but no significant differences compared to *L. sylvaticus*. Pond temperatures are predicted to increase with ongoing climate change over the next 75 years, magnifying the predator performance advantage (ΔV_T) between Agabini beetles and *D. versicolor.* However, the lack of performance differences between predators and *L. sylvaticus* suggests that neither predators nor prey will gain any performance advantages with climate warming.

4.2 Predation pressure may increase for *D. versicolor* but not *L. sylvaticus*

For *D. versicolor*, predator performance advantage, ΔV_T, is predicted to increase through time under all climate scenarios for both surface and bottom water temperatures. Not only do Agabini beetle predators have a performance advantage over *D. versicolor* prey at warm temperatures, but this advantage becomes relatively greater as temperatures approach the beetles T_{opt}. Apart from maximum surface temperatures under the most extreme emissions scenario, climate warming will further advantage predators, with greater impacts at higher emission scenarios.

Relatively greater predator performance could influence the intensity of predator-prey interactions in multiple, direct and indirect, ways. Predation events are composed of three stages: detection, capture, and handling (Dell *et al.* 2014). Of these, increases in relative swim speed differences between Agabini beetles and *D. versicolor* tadpoles are most likely to impact the 'capture' stage. Adult predaceous diving beetles actively chase their prey (Campbell 1969; Culler *et al.* 2014); so, increased relative swim speed should allow predators to catch tadpoles more easily, despite tadpoles also being able to swim faster at higher temperatures. While less obvious than the impact of predator performance advantage on capture success, increases in absolute (rather than relative) predator swim speed could also increase detection of prey by predators. As predator swim speed increases, they will be able to patrol the pond faster and thus have greater chance of detecting tadpoles. This effect may be compounded by the higher absolute swim speed of prey that will also accompany warming. If both predator and prey cover more distance per unit time, then, under an assumption of random movement, they will be more likely to encounter each other, increasing predation opportunities (Dell *et al.* 2014). While I focused on 'burst' swimming to mimic predator escape, unpublished data suggest that higher temperatures can also increase cruising speeds of American Toad (*Anaxyrus americanus*) tadpoles (Bosch and Algar, unpublished data), so it is possible that *D. versicolor* tadpoles may swim faster in warmer water generally, rather than just when fleeing predators. Lastly, if TPCs for swim speed are representative of organism's functional ability more generally (Bennett 1990), then higher temperatures could also reduce prey handling times which could increase predation rates (Dell *et al.* 2014), though

given the small size of Gosner stage 24/25 *D. versicolor* tadpoles, such impacts are likely to be small.

Increases in body temperature induced by higher pond temperatures may also indirectly influence predator-prey interactions, independently of swim speed. As metabolic rate increases with body temperature (Brown *et al.* 2004), both predators and prey require greater food intake to meet energetic demands, thus increasing predation events. For example, experiments on fish have shown increasing attack rates of predators on prey at warmer temperatures (Öhlund *et al.* 2015), consistent with increased predation due to higher metabolic demands. Predation risk may be further impacted by the increased metabolic demands of tadpoles, for whom the act of foraging for more food resources comes with increased risk of being detected by a predator. These effects may be exacerbated by faster growth rates of tadpoles at higher temperatures (Seebacher & Grigaltchik 2014; Zhao *et al.* 2014), which may further increase energetic demands. However, these impacts could be lessened if *D. versicolor* tadpole food resources, i.e. periphyton, become more abundant with warming pond temperatures.

Increased predator performance advantage may also impact *D. versicolor* tadpoles through a 'landscape of fear'. The ‘landscape of fear’ concept describes how predation risk spreads across environments and influences predator and prey behaviours (Hammerschlag *et al.* 2015). In my system, as temperature increases, risk of predation also increases, potentially influencing prey behaviour. Tadpoles facing increased predation risk have been found to decrease their activity and consequently decrease their time spent feeding (Horat & Semlitsch 1994). Therefore, as environmental temperatures increase, metabolic demand increases, and predation risk increases, tadpoles will face a difficult tradeoff, where they

can either decrease activity levels to avoid predation and risk not meeting their metabolic demand or increase activity to meet metabolic demand but risk being predated.

My results suggest that predation pressure will increase on *D. versicolor* tadpoles as pond temperatures warm. By comparing performance capabilities at various temperatures, one can infer how their interactions will play out (Luhring & DeLong 2016; Payne *et al.* 2016; but see Sinclair *et al.* 2016), but it is possible that results from a direct predation rate study would come to different conclusions. However, findings from experimental microcosms suggest that warmer temperatures can lower population sizes of tadpoles from increased predation. For example, De Mira-Mendes *et al.* (2019) found that tadpole mortality of a South American toad (*Rhinella jimi*), due to predation by scavenger beetles (*Hydrophilus*) increased with warmer water temperatures. Similar results have been found for Green Frogs (*Lithobates clamitans)* and larval dragonfly (Odonata) predation (Eck *et al.* 2014), though the impact varied among predator species. Nonetheless, this set of results indicate that tadpoles may face increased predation from a range of insect predators, not just predaceous diving beetles (Dytiscidae). These mesocosm results suggest that effects of enhanced predator performance, and increased predation rate, as temperature increases could scale to the population level and cause prey population declines or local extinctions, though tests are still required to determine if these experimental results transfer to natural systems.

The impacts of warming on predator performance advantage varies among prey species. In contrast to the increases in ΔV_T for *D. versicolor*, for *L. sylvaticus*, ΔV_T, will not increase or decrease through time as their performance was very similar to predators across all temperatures. Although I predict no change in relative swim speed and thus no

effect on the ability of Agabini to pursue *L. sylvaticus* tadpoles, or the ability of the latter to escape, warming could still have impacts through enhancing detection rates or increased metabolic demands as described for *D. versicolor*. Further study is needed to determine whether these mechanisms, even when predator and prey performance are thermally aligned, are strong enough to have broader impacts on prey populations.

The differences in TPCs, and thus ΔV_T, between *L. sylvaticus* and *D. versicolor* could reflect different adaptations to temperature in two species that are in different families (Ranidae and Hylidae, respectively) that themselves are not closely related (Portik *et al.* 2023) but it could also reflect ontogenetic changes. I tested swim speeds of *L. sylvaticus* tadpoles at Gosner stage 27/28, but *D. versicolor* at Gosner stage 25. As tadpoles grow, their swim speed should increase, which may explain why *L. sylvaticus* could match Agabini swim speeds, but *D. versicolor* tadpoles could not. In addition to average swim speed, the shape of the TPC may also shift as tadpoles develop. For example, *L. sylvaticus* tadpole CT_{max} increases as they develop from stages 27-39 and once they reach early metamorphosis (Gosner stage 40), CT_{max} decreases again (Cupp 1980), likewise as in *Rana temporaria* (Ruthsatz *et al.* 2022).

Differences in ΔV_T among species and developmental stages could induce changes in predator behaviour and have impacts on the strength of top-down effects of predators across communities. Prey species with low ΔV_T, like *L. sylvaticus,* are a relatively costly prey type to pursue as they can match the pace of the predator, increasing the energy used in pursuit and decreasing the chance of success. Thus, as temperatures warm, predators may switch to prey, like *D. versicolor*, where ΔV_T has increased, rendering pursuit of these species less costly. Predators may also be more likely to switch to prey at earlier

developmental stages as warming increases. While there is little evidence in beetle-tadpole systems, prey switching can have important implications for broader scales in other taxa; for example, prey switching is predicted to enhance persistence of Canada lynx (*Lynx canadensis*) at their southern range edge (Peers *et al.* 2014). Prey switching may also be exacerbated by differential phenological shifts in predators and prey (e.g. predator-prey mismatch, (Damien & Tougeron 2019) which alter the range of ΔV_T values of prey available to a predator. Direct shifts between *L. sylvaticus* and *D. versicolor* at the Gosner stages studied here are unlikely as these two species are not phenologically aligned (*L. sylvaticus* breed much earlier in the year than *D. versicolor*). However, tadpoles of both species develop in multi-species communities. In my study region, Spring Peepers (*Pseudacris crucifer*) and Boreal Chorus Frogs (*Pseudacris maculata*) breed at similar times as *L. sylvaticus*, followed by Northern Leopard Frogs (*Lithobates pipiens*). American Toads (*Anaxyrus americanus*) breed in the same period as *D. versicolor*, followed by Green Frogs (*Lithobates clamitans*) and Mink Frogs (*Lithobates septentrionalis*) (Dodd 2023). Thus, there is the potential for warming induced changes in ΔV_T to alter the relative strength of predation on these prey species, though this hypothesis needs to be formally tested.

4.3 Thermal performance curve comparisons

I found that *D. versicolor*'s CT_{max} (37.7 ºC ± 2.2) was lower than values reported in the literature: 40.03 ºC ± 0.1 (Katzenberger *et al.* 2021), 41.7 ºC ± 0.1 (Katzenberger *et al.* 2018), and 41.78 ºC ± 0.1 (Katzenberger *et al.* 2014). This could be due to an ensemble of differences: tadpoles were acclimated at different temperatures, were at different developmental stages, and were collected from different parts of their geographic range.

My tadpoles were acclimated at 15 ºC whereas in Katzenberger *et al'*s (2014, 2018, 2021) studies they were acclimated at 20 ºC. Acclimation impacts species thermal performance as it triggers a shift in their thermal physiology, signaling at which temperatures to optimize performance (Lagerspetz 2006). Acclimation temperature has also been found to affect individuals' critical thermal limits, with both CT_{min} and CT_{max} increasing with increased acclimation temperatures (Fan *et al.* 2021). My tadpoles were also only at Gosner stage 25, whereas tadpoles in Katzenberger et al.'s studies were above stage 25 (Katzenberger *et al.* 2021), stage 34 (Katzenberger *et al.* 2018), and stage 38 (Katzenberger *et al.* 2014). Developmental stage has been found to significantly affect CT_{min} and CT_{max} in *Rana temporaria* (Ruthsatz *et al.* 2022), with earlier life stages having a much narrower range of tolerable temperatures (distance between lower and upper thermal limits). Thus, as my tadpoles were younger than tadpoles in other studies, it is possible that their developmental stage was a key reason why their CT_{max} was lower than reference studies. Finally, tadpoles in this study were collected from a latitude of 48.3º in Thunder Bay, Ontario, Canada, while Katzenberger et al.'s animals were collected from and tested at a latitude of 40.4º in Pittsburgh, Pennsylvania, USA. Thunder Bay is close to the northern range edge of *D. versicolor* and has a colder climate than Pennsylvania – with average July temperatures reaching 29 ºC (US Department of Commerce, National Weather Service 2025), the centre of *D. versicolor*'s range (Figure 2.2). Latitude can have variable relationships with intraspecific variation of critical thermal limits. Some species' critical thermal limits increase with latitude, e.g. the Four-eyed Frog, *Pleurodema thaul* (Barria & Bacigalupe 2017), while in others do not, e.g. the Porcelain Crab, *Petrolisthes violaceus* (Gaitán-Espitia *et al.* 2014). However, an effect of latitude on *D. versicolor*

critical thermal limits has yet to be explored, so I can only speculate that latitude plays a role in explaining why the CT_{max} in this study is lower than other literature. To my knowledge, mine is the first reported measure of CT_{min} for *D. versicolor* tadpoles, so comparisons are not possible. The only literature value for T_{opt} and 95% thermal breadth ($T_{br(95\%)}$) of *D. versicolor* tadpoles are 32.5 ± 0.5 ºC and 14.29, respectively (Katzenberger *et al.* 2014). *D. versicolor* in my study had a T_{opt} of 24.2 ± 0.9 ºC, 7.3ºC lower than Katzenberger et al. (2014), and a $T_{br(95\%)}$ of 8.7 ± 0.9, 5.59 narrower than Katzenberger et al. (2014). However, again due to the differences in acclimation, ontogeny, and geographic origin, differences between my results and literature values are not surprising.

For *L. sylvaticus* tadpoles, I experimentally determined that their CT_{max} was 37.2 ºC ± 0.5, a value comparable to other literature values: ~36.5 ºC (Manis & Claussen 1986), 38.2 ºC ± 0.1 (Katzenberger *et al.* 2021), and ~ 37.5 ºC (Cupp 1980). *L. sylvaticus* CT_{min} could not be experimentally determined in this study because we could not cool water sufficiently. The only published CT_{min} of larval *L. sylvaticus* is ~ 4.5 ºC from individuals collected in Minnesota, USA, which were acclimated at 15 ºC (Manis & Claussen 1986). During my experiment, the water temperature reached 3.0 ºC, but tadpoles showed no signs of being near their thermal limit. This suggests that my tadpoles had a much lower thermal limit than what Manis & Claussen (1986) found. The reason for this difference could be ontogeny as the tadpoles in their study were Gosner stage 33-36 and mine were only stage 28. However, this contradicts previous work that found that CT_{min} decreased with increasing age (Ruthsatz *et al.* 2022). The only other difference between my study and Manis & Claussen (1986) is that they used a ramping rate of 0.7 ºC/min whereas I used a rate of 0.25 ± 0.12 ºC/min. Since my ramping rate was slower than Manis &

Claussen (1986), the tadpoles could have had more time to physiologically adjust (partial acclimation) to the decreasing temperature, thus lowering their CT_{min}, though variable (including opposite) effects of ramping rate on critical thermal limits have been documented (Vinagre *et al.* 2015). My ramping rate was, however, comparable with other studies (Cheng *et al.* 2023; Gutiérrez-Pesquera *et al.* 2016; Pintanel *et al.* 2020, 2022). To my knowledge, there are no published estimates of T_{opt} or $T_{br(80\%)}$ for *L. sylvaticus* tadpoles, making my study the first to directly test and report these values.

With respect to the predators, my study is the first, to my knowledge, to directly measure TPCs of Dytiscidae. No other studies have been done on beetle thermal performance, but some have been done on thermal limits of Dytiscidae beetles in southern Australia (Jones *et al.* 2021), southern Africa (Hidalgo-Galiana *et al.* 2021), and Spain (Calosi *et al.* 2008). Jones *et al.* (2021) tested 5 species and found CT_{max}s ranging from 38.2 ± 0.2 ºC – 44.5 ± 0.5 ºC, Hidalgo-Galiana *et al.* (2021) tested 6 species and found CT_{max}s ranging from approximately 40.0 ºC – 44.5 ºC and CT_{min}s ranging from approximately 4.0 ºC – 11.5 ºC, and Calosi *et al.* (2008) tested 4 species and found CT_{max}s ranging from approximately 44.0 ºC – 46.0 ºC and CT_{min}s ranging from approximately -6.5 ºC – -9.0 ºC. Since I was unable to determine CT_{max} or CT_{min} for Agabini beetles in my study, comparisons with the other species from these studies is not possible. .

Predator T_{opt} was significantly greater than *D. versicolor*'s T_{opt}, but not different from *L. sylvaticus*'s. Thus, greater heat adaptation of invertebrate predators than their prey is not a general pattern. Predator $T_{br(80\%)}$ was significantly narrower than both prey species, suggesting that this predator is more of a thermal specialist, and the prey are thermal generalists. Thermal specialists are organisms whose performance is enhanced at a

narrow range of body temperatures, whereas generalists have moderate performance over a broader range of temperatures (Gilchrist 1995). If beetle predators are heat specialists, then climate change will benefit them by raising average environmental temperatures. However, I also found that maximum daily temperatures exceeded the predator's T_{opt} and caused performance and ΔV_T declines, so there is a limit of acceptable environmental warming before predators are negatively affected.

Because CT_{min} and CT_{max} could not be experimentally determined for the beetle predators, comparisons between predators and prey could not be made. Future research should aim to experimentally determine CT_{min} and CT_{max} for these Agabini beetles and aim to better identify when they have reached their critical thermal limits. Likewise with the tadpoles, since I could not experimentally determine the thermal limits for predators, the prey thermal limits were not used to fit TPCs. However, including thermal limits in the dataset when fitting TPCs could help anchor the curves, though the sensitivity of critical thermal limits to ramping rates (Kovacevic *et al.* 2019) could also lead to inaccuracies, as could the fact that they measure responses to temperature over shorter periods than swim experiments.

4.4 Field data and future climate predictions

The close relationship between surface water temperature in ponds and air temperature (Figure 3.12) means that as air temperatures continue to rise through time due to climate change, so will water temperatures. Daily minimum, maximum, and average water temperatures are predicted to increase with time, but differences between surface and bottom water temperatures offer more complex thermal environments, providing opportunities for behavioural thermoregulation. Since the bottom of the pond is colder

than the surface, tadpoles may be able to hide in the cooler water to avoid active predators, however, this comes with trade-offs as there may be limited food resources and growth rates are slower in colder temperatures (Seebacher & Grigaltchik 2014; Zhao *et al.* 2014). However, if tadpoles remain in warmer water near the surface of the pond they optimize growth and might outgrow the beetle predators but risk being predated while they are still developing.

Finally, pond temperatures are predicted to increase significantly through time (Figure 3.14 and Figure 3.15), and *D. versicolor* prey actually gain an advantage at the extremely high temperatures of the highest emissions scenario (Figure 3.16). However, such high temperatures may occur over only very short periods. It is also maybe that the hottest temperatures predicted by my model may be physically impossible due to evaporation. Evapotranspiration from the pond surface and nearby vegetation is the major pathway of water loss from ponds and is highly influenced by temperature (Brooks 2004, 2005). As water warms, it undergoes more evaporative cooling, which means that water molecules leave as gas and take energy (heat) with them (Harman 2005). So, as pond temperatures increase, evaporative cooling will take effect and decrease the temperature, setting an upper limit of the possible temperatures and causing ponds to dry up faster. This could have dual impacts on tadpoles; warming may increase predation risk for some species, while faster drying may prevent them from reaching metamorphosis resulting in mortality of the whole clutch (Newman 1992), or metamorphosizing sooner, at smaller size, potentially reducing adult fitness (Francesco Ficetola & De Bernardi 2006).

4.5 Conclusions

In summary, Agabini beetle predators were more heat adapted than *D. versicolor* tadpoles but not *L. sylvaticus* tadpoles, showing variability between predator-prey pairs in the same environment. Predators having a performance advantage over their prey may result in increased predation pressure and could reduce prey populations. As climate change increases future air temperatures, pond water temperatures will also increase. This change in thermal regime will alter predator-prey interactions, but not between all predator-prey pairs. Further research should aim to develop better measures of Dytiscidae (tribe: Agabini) critical thermal limits. Also, more investigation into how ontogeny influences these predator-prey interactions is required to fully understand how climate warming will affect the vulnerable species in these small, but complex, aquatic environments.

5 References

Allan, B.J.M., Domenici, P., Munday, P.L. & McCormick, M.I. (2015). Feeling the heat: the effect of acute temperature changes on predator–prey interactions in coral reef fish. *Conserv. Physiol.*, 3, cov011.

Anderson, M.T., Kiesecker, J.M., Chivers, D.P. & Blaustein, A.R. (2001). The direct and indirect effects of temperature on a predator–prey relationship. *Can. J. Zool.*, 79, 1834–1841.

Angilletta, M.J. (2009). *Thermal adaptation: a theoretical and empirical synthesis.* Oxford University Press.

Barria, A.M. & Bacigalupe, L.D. (2017). Intraspecific geographic variation in thermal limits and acclimatory capacity in a wide distributed endemic frog. *J. Therm. Biol.*, 69, 254–260.

Beachy, C.K., Surges, T.H. & Reyes, M. (1999). Effects of developmental and growth history on metamorphosis in the gray treefrog,Hyla versicolor (Amphibia, Anura). *J. Exp. Zool.*, 283, 522–530.

Beltran, I. (2019). Dealing with hot rocky environments: Critical thermal maxima and locomotor performance in Leptodactylus lithonaetes (Anura: Leptodactylidae). *Herpetol. J.*, 155–161.

Bennett, A.F. (1990). Thermal dependence of locomotor capacity. *Am. J. Physiol.-Regul. Integr. Comp. Physiol.*, 259, R253–R258.

Bideault, A., Galiana, N., Zelnik, Y.R., Gravel, D., Loreau, M., Barbier, M., *et al.* (2021). Thermal mismatches in biological rates determine trophic control and biomass distribution under warming. *Glob. Change Biol.*, 27, 257–269.

Bragg, A.N. (1957). Variation in Colors and Color Patterns in Tadpoles in Oklahoma. *Copeia*, 1957, 36.

Broitman, B.R., Szathmary, P.L., Mislan, K.A.S., Blanchette, C.A. & Helmuth, B. (2009). Predator–prey interactions under climate change: the importance of habitat vs body temperature. *Oikos*, 118, 219–224.

Brooks, R.T. (2004). Weather-related effects on woodland vernal pool hydrology and hydroperiod. *Wetlands*, 24, 104–114.

Brooks, R.T. (2005). A review of basin morphology and pool hydrology of isolated ponded wetlands: implications for seasonal forest pools of the northeastern United States. *Wetl. Ecol. Manag.*, 13, 335–348.

Brooks, R.T. & Hayashi, M. (2002). Depth-area-volume and hydroperiod relationships of ephemeral (vernal) forest pools in southern New England. *Wetlands*, 22, 247–255.

Brown, D., Hanson, R. & Christian, W. (2025). Tracker Video Analysis and Modeling Tool (Version 6.2.0).

Brown, J.H., Gillooly, J.F., Allen, A.P., Savage, V.M. & West, G.B. (2004). Toward a metabolic theory of ecology. *Ecology*, 85, 1771–1789.

Buckley, L.B. & Huey, R.B. (2016). How Extreme Temperatures Impact Organisms and the Evolution of their Thermal Tolerance. *Integr. Comp. Biol.*, 56, 98–109.

Buckley, L.B., Huey, R.B. & Kingsolver, J.G. (2022). Asymmetry of thermal sensitivity and the thermal risk of climate change. *Glob. Ecol. Biogeogr.*, 31, 2231–2244.

Calosi, P., Bilton, D.T., Spicer, J.I. & Atfield, A. (2008). Thermal tolerance and geographical range size in the *Agabus brunneus* group of European diving beetles (Coleoptera: Dytiscidae). *J. Biogeogr.*, 35, 295–305.

Campbell, A. (1969). The predatory behaviour of the larvae of *colymbetes sculpttlis* (harris) and *graphoderus occtdentalis* horn (coleopteira: dytisctdae).
Cano, J.M. & Nicieza, A.G. (2006). Temperature, metabolic rate, and constraints on locomotor performance in ectotherm vertebrates. *Funct. Ecol.*, 20, 464–470.
Careau, V., Killen, S.S. & Metcalfe, N.B. (2014). Adding Fuel to the "Fire of Life": Energy Budgets across Levels of Variation in Ectotherms and Endotherms. In: *Integrative Organismal Biology* (eds. Martin, L.B., Ghalambor, C.K. & Woods, H.A.). Wiley, pp. 219–233.
Cartwright, J., Morelli, T.L. & Grant, E.H.C. (2021). Identifying climate-resistant vernal pools: Hydrologic refugia for amphibian reproduction under droughts and climate change. *Ecohydrology*, 15, e2354.
Cheng, C., Chuang, M., Haramura, T., Cheng, C., Kim, Y.I., Borzée, A., *et al.* (2023). Open habitats increase vulnerability of amphibian tadpoles to climate warming across latitude. *Glob. Ecol. Biogeogr.*, 32, 83–94.
Clusella-Trullas, S., Garcia, R.A., Terblanche, J.S. & Hoffmann, A.A. (2021). How useful are thermal vulnerability indices? *Trends Ecol. Evol.*, 36, 1000–1010.
Crins, W.J., Gray, P.A., Uhlig, P.W.C. & Wester, M.C. (2009). The Ecosystems of Ontario, Part 1: Ecozones and Ecoregions. *Ont. Minist. Nat. Resour.*
Culler, L.E., McPeek, M.A. & Ayres, M.P. (2014). Predation risk shapes thermal physiology of a predaceous damselfly. *Oecologia*, 176, 653–660.
Cupp, P.V. (1980). Thermal Tolerance of Five Salientian Amphibians during Development and Metamorphosis. *Herpetologica*, 36, 234–244.
Damien, M. & Tougeron, K. (2019). Prey–predator phenological mismatch under climate change. *Curr. Opin. Insect Sci.*, 35, 60–68.
Davidson, A.T., Hamman, E.A., McCoy, M.W. & Vonesh, J.R. (2021). Asymmetrical effects of temperature on stage-structured predator–prey interactions. *Funct. Ecol.*, 35, 1041–1054.
De Mira-Mendes, C.V., Costa, R.N., Dias, I.R., Carilo Filho, L.M., Mariano, R., Le Pendu, Y., *et al.* (2019). Effects of increasing temperature on predator-prey interaction between beetle larvae and tadpoles. *Stud. Neotropical Fauna Environ.*, 54, 163–168.
Dell, A.I., Pawar, S. & Savage, V.M. (2014). Temperature dependence of trophic interactions are driven by asymmetry of species responses and foraging strategy. *J. Anim. Ecol.*, 83, 70–84.
Deutsch, C.A., Tewksbury, J.J., Huey, R.B., Sheldon, K.S., Ghalambor, C.K., Haak, D.C., *et al.* (2008). Impacts of climate warming on terrestrial ectotherms across latitude. *Proc. Natl. Acad. Sci.*, 105, 6668–6672.
Dodd, K.C. (2023). *Frogs of the United States and Canada*. 2nd edn. John Hopkins University Press., Baltimore.
Eck, B., Byrne, A., Popescu, V.D., Harper, E.B. & Patrick, D.A. (2014). Effects of water temperature on larval amphibian predator-prey dynamics. *Herpetol. Conserv. Biol.*, 9, 302–308.
Fan, X.L., Lin, Z.H. & Scheffers, B.R. (2021). Physiological, developmental, and behavioral plasticity in response to thermal acclimation. *J. Therm. Biol.*, 97, 102866.

Fiala, A.C.S., Garman, S.L. & Gray, A.N. (2006). Comparison of five canopy cover estimation techniques in the western Oregon Cascades. *For. Ecol. Manag.*, 232, 188–197.
Francesco Ficetola, G. & De Bernardi, F. (2006). Trade-off between larval development rate and Post-metamorphic Traits in the Frog Rana latastei. *Evol. Ecol.*, 20, 143–158.
Freitas, V., Campos, J., Fonds, M. & Van Der Veer, H.W. (2007). Potential impact of temperature change on epibenthic predator–bivalve prey interactions in temperate estuaries. *J. Therm. Biol.*, 32, 328–340.
Gaitán-Espitia, J.D., Bacigalupe, L.D., Opitz, T., Lagos, N.A., Timmermann, T. & Lardies, M.A. (2014). Geographic variation in thermal physiological performance of the intertidal crab *Petrolisthes violaceus* along a latitudinal gradient. *J. Exp. Biol.*, jeb.108217.
Gates, D.M. (1980). *Biophysical Ecology*. 1st edn. Springer New York, NY, New York.
Ge, X., Griswold, C.K. & Newman, J.A. (2022). *Predator-prey interactions in a warming world: the critical role of cold tolerance* (preprint). Ecology.
Gilchrist, G.W. (1995). Specialists and Generalists in Changing Environments. I. Fitness Landscapes of Thermal Sensitivity. *Am. Nat.*, 146, 252–270.
Gilman, S.E., Urban, M.C., Tewksbury, J., Gilchrist, G.W. & Holt, R.D. (2010). A framework for community interactions under climate change. *Trends Ecol. Evol.*, 25, 325–331.
Grigaltchik, V.S., Ward, A.J.W. & Seebacher, F. (2012). Thermal acclimation of interactions: differential responses to temperature change alter predator–prey relationship.
Guderley, H. (2004). Metabolic responses to low temperature in fish muscle. *Biol. Rev.*, 79, 409–427.
Gutiérrez-Pesquera, L.M., Tejedo, M., Olalla-Tárraga, M.Á., Duarte, H., Nicieza, A. & Solé, M. (2016). Testing the climate variability hypothesis in thermal tolerance limits of tropical and temperate tadpoles. *J. Biogeogr.*, 43, 1166–1178.
Gvoždík, L. (2018). Just what is the thermal niche? *Oikos*, 127, 1701–1710.
Gvoždík, L. & Smolinský, R. (2015). Body size, swimming speed, or thermal sensitivity? Predator-imposed selection on amphibian larvae. *BMC Evol. Biol.*, 15, 238.
Häder, D.-P. & Barnes, P.W. (2019). Comparing the impacts of climate change on the responses and linkages between terrestrial and aquatic ecosystems. *Sci. Total Environ.*, 682, 239–246.
Hammerschlag, N., Broderick, A.C., Coker, J.W., Coyne, M.S., Dodd, M., Frick, M.G., *et al.* (2015). Evaluating the landscape of fear between apex predatory sharks and mobile sea turtles across a large dynamic seascape. *Ecology*, 96, 2117–2126.
Harding, J. & Mifsud, D. (2017). *Amphibians and Reptiles of the Great Lakes Region.* University of Michigan Press, Ann Arbor, MI, USA.
Harman, R. (2005). *The Water Cycle: Evaporation Condensation and Erosion.* Heinemann Librar, Chicago, IL, USA.
Hartig, F. (2024). DHARMa: Residual Diagnostics for Hierarchical (Multi-Level/Mixed) Regression Models.
Hidalgo-Galiana, A., Ribera, I. & Terblanche, J.S. (2021). Geographic variation in acclimation responses of thermal tolerance in South African diving beetles

(Dytiscidae: Coleoptera). *Comp. Biochem. Physiol. A. Mol. Integr. Physiol.*, 257, 110955.
HilleRisLambers, J., Harsch, M.A., Ettinger, A.K., Ford, K.R. & Theobald, E.J. (2013). How will biotic interactions influence climate change–induced range shifts? *Ann. N. Y. Acad. Sci.*, 1297, 112–125.
Hilsenhoff, W.L. (1993). Dytiscidae and Noteridae of Wisconsin (Coleoptera). IV. Distribution, Habitat, Life Cycle, and Identification of Species of Agabini (Colymbetinae). *Gt. Lakes Entomol.*, 26, 173–197.
Hocking, D.J. & Semlitsch, R.D. (2008). Effects of Experimental Clearcut Logging on Gray Treefrog (Hyla versicolor) Tadpole Performance. *J. Herpetol.*, 42, 689–698.
Holden, Z.A., Klene, A.E., F. Keefe, R. & G. Moisen, G. (2013). Design and evaluation of an inexpensive radiation shield for monitoring surface air temperatures. *Agric. For. Meteorol.*, 180, 281–286.
Horat, P. & Semlitsch, R.D. (1994). Effects of predation risk and hunger on the behaviour of two species of tadpoles. *Behav. Ecol. Sociobiol.*, 34, 393–401.
Huey, R.B. & Kingsolver, J.G. (2019). Climate Warming, Resource Availability, and the Metabolic Meltdown of Ectotherms. *Am. Nat.*, 194, E140–E150.
Jefferson, D.M., Hobson, K.A. & Chivers, D.P. (2014). Time to feed: How diet, competition, and experience may influence feeding behaviour and cannibalism in wood frog tadpoles Lithobates sylvaticus. *Curr. Zool.*, 60, 571–580.
Jones, K.K., Humphreys, W.F., Saccò, M., Bertozzi, T., Austin, A.D. & Cooper, S.J.B. (2021). The critical thermal maximum of diving beetles (Coleoptera: Dytiscidae): a comparison of subterranean and surface-dwelling species. *Curr. Res. Insect Sci.*, 1, 100019.
Katzenberger, M., Duarte, H., Relyea, R., Beltrán, J.F. & Tejedo, M. (2021). Variation in upper thermal tolerance among 19 species from temperate wetlands. *J. Therm. Biol.*, 96, 102856.
Katzenberger, M., Hammond, J., Duarte, H., Tejedo, M., Calabuig, C. & Relyea, R.A. (2014). Swimming with Predators and Pesticides: How Environmental Stressors Affect the Thermal Physiology of Tadpoles. *PLoS ONE*, 9, e98265.
Katzenberger, M., Hammond, J., Tejedo, M. & Relyea, R. (2018). Source of environmental data and warming tolerance estimation in six species of North American larval anurans. *J. Therm. Biol.*, 76, 171–178.
Kern, P., Cramp, R.L. & Franklin, C.E. (2015). Physiological responses of ectotherms to daily temperature variation. *J. Exp. Biol.*, jeb.123166.
Kovacevic, A., Latombe, G. & Chown, S.L. (2019). Rate dynamics of ectotherm responses to thermal stress. *Proc. R. Soc. B Biol. Sci.*, 286, 20190174.
Lagerspetz, K.Y.H. (2006). What is thermal acclimation? *J. Therm. Biol.*, 31, 332–336.
Leibowitz, S.G. & Brooks, R.T. (2007). Hydrology and Landscape Connectivity of Vernal Pools. *Sci. Conserv. Vernal Pools Northeast. N. Am.*, 32–51.
Luhring, T.M. & DeLong, J.P. (2016). Predation changes the shape of thermal performance curves for population growth rate. *Curr. Zool.*, 62, 501–505.
Lutterschmidt, W.I. & Hutchison, V.H. (1997). The critical thermal maximum: history and critique. *Can. J. Zool.*, 75, 1561–1574.

Ma, G., Bai, C.-M., Wang, X.-J., Majeed, M.Z. & Ma, C.-S. (2018). Behavioural thermoregulation alters microhabitat utilization and demographic rates in ectothermic invertebrates. *Anim. Behav.*, 142, 49–57.
Manis, M.L. & Claussen, D.L. (1986). Environmental and genetic influences on the thermal physiology of Rana sylvatica. *J. Therm. Biol.*, 11, 31–36.
McDiarmid, R.W. & Altig, R. (1999). *Tadpoles: the biology of anuran larvae.* University of Chicago Press.
Meehan, M.L. & Lindo, Z. (2023). Mismatches in thermal performance between ectothermic predators and prey alter interaction strength and top-down control. *Oecologia*, 201, 1005–1015.
Montoya, J.M. & Raffaelli, D. (2010). Climate change, biotic interactions and ecosystem services. *Philos. Trans. R. Soc. B Biol. Sci.*, 365, 2013–2018.
Morley, S.A., Peck, L.S., Sunday, J.M., Heiser, S. & Bates, A.E. (2019). Physiological acclimation and persistence of ectothermic species under extreme heat events. *Glob. Ecol. Biogeogr.*, 28, 1018–1037.
Nagano, K., Hiraiwa, M.K., Ishiwaka, N., Seko, Y., Hashimoto, K., Uchida, T., *et al.* (2023). Global warming intensifies the interference competition by a poleward-expanding invader on a native dragonfly species. *R. Soc. Open Sci.*, 10, 230449.
Newman, R.A. (1992). Adaptive Plasticity in Amphibian Metamorphosis. *BioScience*, 42, 671–678.
Ohba, S. (2011). Density-Dependent Effects of Amphibian Prey on the Growth and Survival of an Endangered Giant Water Bug. *Insects*, 2, 435–446.
Öhlund, G., Hedström, P., Norman, S., Hein, C.L. & Englund, G. (2015). Temperature dependence of predation depends on the relative performance of predators and prey. *Proc. R. Soc. B Biol. Sci.*, 282, 20142254.
Padfield, D. & O'Sullivan, H. (2023). rTPC: Fitting and Analysing Thermal Performance Curves.
Parmesan, C. & Yohe, G. (2003). A globally coherent fingerprint of climate change impacts across natural systems. *Nature*, 421, 37–42.
Payne, N.L., Smith, J.A., Van Der Meulen, D.E., Taylor, M.D., Watanabe, Y.Y., Takahashi, A., *et al.* (2016). Temperature dependence of fish performance in the wild: links with species biogeography and physiological thermal tolerance. *Funct. Ecol.*, 30, 903–912.
Peers, M.J.L., Wehtje, M., Thornton, D.H. & Murray, D.L. (2014). Prey switching as a means of enhancing persistence in predators at the trailing southern edge. *Glob. Change Biol.*, 20, 1126–1135.
Perotti, M.G., Bonino, M.F., Ferraro, D. & Cruz, F.B. (2018). How sensitive are temperate tadpoles to climate change? The use of thermal physiology and niche model tools to assess vulnerability. *Zoology*, 127, 95–105.
Petchey, O.L., Brose, U. & Rall, B.C. (2010). Predicting the effects of temperature on food web connectance. *Philos. Trans. R. Soc. B Biol. Sci.*, 365, 2081–2091.
Pierce, D. (2025). ncdf4: Interface to Unidata netCDF (Version 4 or Earlier)Format Data Files.
Pintanel, P., Tejedo, M., Almeida-Reinoso, F., Merino-Viteri, A. & Gutiérrez-Pesquera, L.M. (2020). Critical Thermal Limits Do Not Vary between Wild-caught and Captive-bred Tadpoles of Agalychnis spurrelli (Anura: Hylidae). *Diversity*, 12, 43.

Pintanel, P., Tejedo, M., Merino-Viteri, A., Almeida-Reinoso, F., Salinas-Ivanenko, S., López-Rosero, A.C., *et al.* (2022). Elevational and local climate variability predicts thermal breadth of mountain tropical tadpoles. *Ecography*, 2022, e05906.

Pintanel, P., Tejedo, M., Salinas, S., Jervis, P. & Merino, A. (2021). Predators like it hot: Thermal mismatch in a predator–prey system across an elevational tropical gradient. *J. Anim. Ecol.*, 90, 1985–1995.

Poloczanska, E.S., Brown, C.J., Sydeman, W.J., Kiessling, W., Schoeman, D.S., Moore, P.J., *et al.* (2013). Global imprint of climate change on marine life. *Nat. Clim. Change*, 3, 919–925.

Portik, D.M., Streicher, J.W. & Wiens, J.J. (2023). Frog phylogeny: A time-calibrated, species-level tree based on hundreds of loci and 5,242 species. *Mol. Phylogenet. Evol.*, 188, 107907.

Relyea, R.A. (2001). Morphological and behavioral plasticity of larval anurans in response to different predators. *Ecology*, 82, 523–540.

Relyea, R.A. (2018). The interactive effects of predator stress, predation, and the herbicide Roundup. *Ecosphere*, 9, e02476.

Relyea, R.A. (2024). Local Population Differences in Phenotypic Plasticity: Predator-Induced Changes in Wood Frog Tadpoles, 72.

Rezende, E.L. & Bozinovic, F. (2019). Thermal performance across levels of biological organization. *Philos. Trans. R. Soc. B Biol. Sci.*, 374, 20180549.

Ruthsatz, K., Dausmann, K.H., Peck, M.A. & Glos, J. (2022). Thermal tolerance and acclimation capacity in the European common frog (*Rana temporaria*) change throughout ontogeny. *J. Exp. Zool. Part Ecol. Integr. Physiol.*, 337, 477–490.

Ruxton, G.D. & Neuhäuser, M. (2013). Improving the reporting of *P*-values generated by randomization methods. *Methods Ecol. Evol.*, 4, 1033–1036.

Savva, I., Bennett, S., Roca, G., Jordà, G. & Marbà, N. (2018). Thermal tolerance of Mediterranean marine macrophytes: Vulnerability to global warming. *Ecol. Evol.*, 8, 12032–12043.

Schindler, D.W. (1998). A Dim Future for Boreal Waters and Landscapes. *BioScience*, 48, 157–164.

Schneider, C.A., Rasband, W.S. & Eliceiri, K.W. (2012). NIH Image to ImageJ: 25 years of image analysis. *Nat. Methods*, 9, 671–675.

Schock, D.M. (2009). Amphibian population and pathogen surveys in the dehcho and sahtu, northwest territories, 2007 AND 2008. *Dep. Environ. Nat. Resour. Gov. N. W. T.*

Schoeppner, N.M. & Relyea, R.A. (2009). Interpreting the smells of predation: how alarm cues and kairomones induce different prey defences. *Funct. Ecol.*, 23, 1114–1121.

Seebacher, F. & Grigalchik, V.S. (2015). Developmental thermal plasticity of prey modifies the impact of predation. *J. Exp. Biol.*, jeb.116558.

Seebacher, F. & Grigaltchik, V.S. (2014). Embryonic Developmental Temperatures Modulate Thermal Acclimation of Performance Curves in Tadpoles of the Frog Limnodynastes peronii. *PLoS ONE*, 9, e106492.

Sentis, A., Hemptinne, J.-L. & Brodeur, J. (2012). Using functional response modeling to investigate the effect of temperature on predator feeding rate and energetic efficiency. *Oecologia*, 169, 1117–1125.

Shaffery, H.M. & Relyea, R.A. (2016). Dissecting the smell of fear from conspecific and heterospecific prey: investigating the processes that induce anti-predator defenses. *Oecologia*, 180, 55–65.
Sinclair, B.J., Marshall, K.E., Sewell, M.A., Levesque, D.L., Willett, C.S., Slotsbo, S., *et al.* (2016). Can we predict ectotherm responses to climate change using thermal performance curves and body temperatures? *Ecol. Lett.*, 19, 1372–1385.
Strickler, G.S. (1959). Use of the densiometer to estimate density o f forest canopy on permanent sample plots. *US Dep. Agric. Res. Note*.
Sunday, J.M., Bates, A.E., Kearney, M.R., Colwell, R.K., Dulvy, N.K., Longino, J.T., *et al.* (2014). Thermal-safety margins and the necessity of thermoregulatory behavior across latitude and elevation. *Proc. Natl. Acad. Sci.*, 111, 5610–5615.
Tracy, C.R. (1976). A Model of the Dynamic Exchanges of Water and Energy between a Terrestrial Amphibian and Its Environment. *Ecol. Monogr.*, 46, 293–326.
Trembath, R. & Anholt, B.R. (2001). Predator-induced morphological and behavioral changes in a temporary pool vertebrate. *Isr. J. Zool.*, 47, 419–431.
Twardochleb, L.A., Treakle, T.C. & Zarnetske, P.L. (2020). Foraging strategy mediates ectotherm predator–prey responses to climate warming. *Ecology*, 101, e03146.
US Department of Commerce, National Weather Service. (2025). NWS Pittsburgh climate page.
Vinagre, C., Leal, I., Mendonça, V. & Flores, A.A.V. (2015). Effect of warming rate on the critical thermal maxima of crabs, shrimp and fish. *J. Therm. Biol.*, 47, 19–25.
Xu, W., Wang, Y., Wang, G., Zhang, L., Zhang, G., Huo, Z., *et al.* (2024). Heritability Estimates for Growth Traits and Correlation Analysis between Weight and Metamorphosis Rate in the Bullfrog Rana (Aquarana) catesbeiana. *Fishes*, 9, 105.
Zhao, J., Yang, Y., Xi, X., Zhang, C. & Sun, S. (2014). Artificial Warming Facilitates Growth but Not Survival of Plateau Frog (Rana kukunoris) Tadpoles in Presence of Gape-Limited Predatory Beetles. *PLoS ONE*, 9, e98252.

6 Appendix

Appendix A – 2024 Pond temperatures

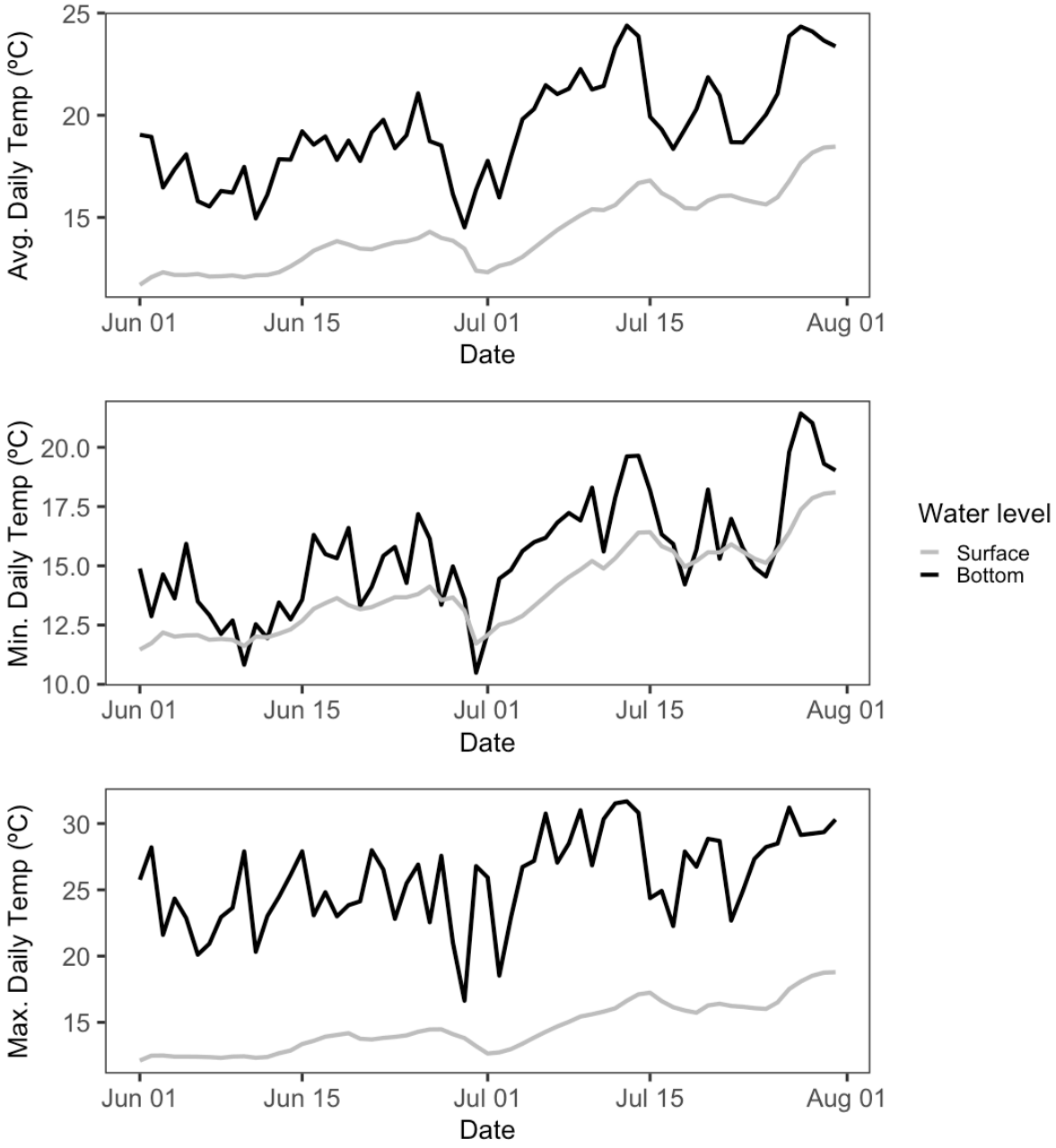

Figure 6.1. (Top) Daily average pond temperatures for June and July 2024. (Middle) Daily minimum pond temperatures for June and July 2024. (Bottom) Daily maximum pond temperatures for June and July 2024. Black line shows the surface water temperatures and grey line shows the temperature of the bottom of the pond.

Appendix B – Generalized linear model assumptions tests

Table 6.1. Results from DHARMa GLM assumptions tests (Hartig 2024). To pass the assumption test, p-values should not be <0.05.

	DHARMa tests			
Model	Quantiles	Uniformity	Dispersion	Outliers
glm(Avg surface temp ~ Avg air temp) Gamma, link = sqrt	$p = 0.7296$	$p = 0.9997$	$p = 0.832$	0 / 61
glm(Min surface temp ~ Min air temp) Gamma, link = sqrt	$p = 0.8914$	$p = 0.8599$	$p = 0.984$	0 / 61
glm(Max surface temp ~ Max air temp) Gamma, link = sqrt	$p = 0.08506$	$p = 0.2343$	$p = 0.68$	0 / 61
glm(Avg bottom temp ~ Avg surface temp) Gamma, link = log	$p = 0.5332$	$p = 0.9461$	$p = 0.936$	0 / 61
glm(Min bottom temp ~ Min surface temp) Gamma, link = log	$p = 0.6055$	$p = 0.5326$	$p = 0.856$	0 / 61
glm(Max bottom temp ~ Max surface temp) Gamma, link = sqrt	$p = 0.06876$	$p = 0.8772$	$p = 0.768$	0 / 61